Modeling for Land Surface Temperature Change in Taiwan

Sahidan Abdulmana

A Thesis Submitted in Fulfillment of the Requirements for the Degree of Doctor of Philosophy in Research Methodology

Prince of Songkla University

2022

Modeling for Land Surface Temperature Change in Taiwan

Sahidan Abdulmana

A Thesis Submitted in Fulfillment of the Requirements for the Degree of Doctor of Philosophy in Research Methodology

Prince of Songkla University

2022

Thesis Title	Modeling for Land Surface Temperature Change in Taiwan
Author	Mr. Sahidan Abdulmana
Major Program	Research Methodology

Major Advisor:

…………………………….................

(Assoc. Prof. Dr. Apiradee Lim)

Co- advisors:

Don McNeil

…………………………….................

(Emeritus Prof. Dr. Don McNeil)

Examining Committee:

…………………………...…… Chairperson

(Asst. Prof. Dr.Wandee Wanishsakpong)

....Committee

(Asst. Prof. Dr. Rhysa McNeil)

....Committee

(Asst. Prof. Dr. Mayuening Eso)

....Committee

(Assoc. Prof. Dr. Apiradee Lim)

Don McNeil

....Committee

(Emeritus Prof. Dr. Don McNeil)

The Graduate School, Prince of Songkla University, has approved this thesis as fulfilment of the requirements for the Doctor of Philosophy Degree in Research Methodology.

……………………………...………

(Prof. Dr. Damrongsak Faroongsarng)

Dean of Graduate School

This is to certify that the work here submitted is the result of the candidate's own investigations. Due acknowledgement has been made of any assistance received.

………..…………………………….Signature

(Assoc. Prof. Dr. Apiradee Lim)

Major Advisor

………..…………………………….Signature

(Mr. Sahidan Abdulmana)

Candidate

I hereby certify that this work has not been accepted in substance for any degree, and is not being currently submitted in candidature for any degree.

...……………………………….Signature

(Mr. Sahidan Abdulmana)

Candidate

ชื่อวิทยานิพนธ์ การสร้างตัวแบบการเปลี่ยนแปลงของอุณหภูมิพื้นผิวในประเทศไต้หวัน

ผู้เขียน นายสาฮีดัน อับดุลมานะ

สาขาวิชา วิธีวิทยาการวิจัย

ปีการศึกษา 2564

บทคัดย่อ

อุณหภูมิพื้นผิว (land surface temperature) เป็นปัจจัยที่สำคัญในการศึกษาความสมดุลของพลังงานพื้นผิวและการศึกษาภูมิอากาศของโลก ลักษณะของอุณหภูมิพื้นผิว เช่น ระดับความสูงของพื้นที่ (elevation) พื้นที่ปกคลุม (land cover) และดัชนีพืชพรรณ (vegetation) สามารถส่งผลต่อการเปลี่ยนแปลงของอุณหภูมิพื้นผิวได้อย่างมีนัยสำคัญ การศึกษานี้มีวัตถุประสงค์เพื่อศึกษารูปแบบการเปลี่ยนแปลงของอุณหภูมิพื้นผิวตามฤดูกาล แนวโน้มการเปลี่ยนแปลงในทศวรรษ ความสัมพันธ์ และรูปแบบการการเปลี่ยนแปลงของอุณหภูมิพื้นผิวและดัชนีพืชพรรณตามประเภทพื้นที่ปกคลุม และเพื่อศึกษาผลกระทบของความแปรผันของพื้นที่ปกคลุมและระดับความสูงของพื้นที่มีผลต่อการเปลี่ยนแปลงของอุณหภูมิพื้นผิวในประเทศไต้หวันโดยใช้ผลรวมถ่วงน้ำหนักการถดถอยเชิงเส้นของ (weighted sum contrasts linear regression) ข้อมูลอุณหภูมิพื้นผิวดัชนีพืชพรรณและพื้นที่ปกคลุมดาวน์โหลดจาก MODIS Land Product (ORNL DAAC, 2018) เว็บไซต์ และข้อมูลระดับความสูงของพื้นที่ดาวน์โหลดจาก USGS Earth Explorer เว็บไซต์ Natural cubic spline และ Multivariate linear regression ใช้เพื่อจำลองรูปแบบการเปลี่ยนแปลงตามฤดูกาล แนวโน้มช่วงทศวรรษ และอัตราเร่งการเปลี่ยนแปลงต่อประเภทของพื้นที่ปกคลุมสุดท้ายนำผลรวมถ่วงน้ำหนักที่ตัดกันของสมการการถดถอยเชิงเส้นมาใช้เพื่อศึกษาผลกระทบของการเปลี่ยนแปลงพื้นที่ปกคลุมและระดับความสูงต่อการเปลี่ยนแปลงของอุณหภูมิ

พื้นผิวต่อทศวรรษ ผลการวิจัยพบว่าพื้นที่แห้งแล้ง (BB land) มีอุณหภูมิเพิ่มขึ้นอย่างมีนัยสำคัญ (0.862°C ต่อทศวรรษ) การเพิ่มขึ้นของอุณหภูมิพื้นผิวและดัชนีพืชพรรณในเวลากลางวันเฉลี่ยอยู่ที่ 0.141°C และ 0.019 หน่วยต่อทศวรรษตามลำดับ นอกจากนี้ประเทศไต้หวันมีแนวโน้มเฉลี่ยของดัชนีพืชพรรณที่เพิ่มขึ้นต่อทศวรรษแต่ไม่ใช่อุณหภูมิพื้นผิว อุณหภูมิพื้นผิวและดัชนีพืชพรรณมีความสัมพันธ์เชิงลบและมีนัยสำคัญต่อพื้นที่สีเขียวเมื่อเทียบกับพื้นที่พักอาศัย (build-up area) ในส่วนระดับพื้นที่พบว่าการเพิ่มขึ้นของอุณหภูมิพื้นผิวและการลดลงของดัชนีพืชพรรณมีจำนวนมากที่ระดับความสูงที่เป็นเทือกเขาสูงซึ่งตั้งอยู่ทางตอนใต้ของประเทศแต่ในระดับพิกเซลการขยายตัวของเมืองและพื้นที่การเกษตรทำให้อุณหภูมิพื้นผิวเพิ่มขึ้นในขณะที่การปลูกป่ามีส่วนทำให้อุณหภูมิลดลง นอกจากนี้การศึกษายังระบุด้วยว่ารูปแบบที่หลากหลายของการแปรผันของพื้นที่ปกคลุมมีอิทธิพลอย่างมากต่อการเปลี่ยนแปลงอุณหภูมิพื้นผิวในเวลากลางวันแต่ไม่ใช่เวลากลางคืน ระดับความสูงที่สูงกว่า 600 ม. มีผลกระทบต่ออุณหภูมิพื้นผิวทั้งกลางวันและกลางคืน อย่างไรก็ตามอัตราการเพิ่มขึ้นของพื้นที่สีเขียวยังไม่ลดลงหน่วยงานที่รับผิดชอบไม่ว่าจะเป็นหน่วยงานกำหนดนโยบายและหน่วยงานที่เกี่ยวข้องต้องมีการวางแผนและพิจารณาเพื่อเป็นเมืองสีเขียวและรับมือกับสภาวะอุณหภูมิที่เพิ่มขึ้น

Thesis title Modeling for Land Surface Temperature Change in Taiwan

Author Mr. Sahidan Abdulmana

Major program Research Methodology

Academic Year 2021

ABSTRACT

Land surface temperature (LST) is an important factor in surface energy balance and global climatology studies. LST characteristics such as elevation, land cover (LC) and vegetation can significantly affect LST. This study aimed to investigate the annual seasonal patterns, decadal trends, their relationships, and dynamic acceleration patterns in LST and NDVI changes through diverse LC types and to examine the influence of LC variation and elevation on LST in a decadal trend in Taiwan by using weighted sum contrasts linear regression. LST, NDVI and LC data were retrieved from the MODIS Land Product subset tool (ORNL DAAC, 2018) and elevation data were downloaded from the USGS Earth Explorer website. The natural cubic spline method and multivariate linear regression were used to model annual seasonal patterns, decadal trends, and acceleration rates for each LU type. Acceleration patterns were analyzed using the correlations between derived trends and acceleration rates. Finally, weighted sum contrasts linear regression was applied to evaluate the influence of LC alteration and elevation on the decadal change of LST. Results showed that BB land had a significant increase in LST (0.862°C per decade). The average increase in daytime LST and NDVI were 0.141°C and 0.019 unit per decade, respectively. Moreover, Taiwan had a significant mean increase in decadal trends of NDVI but not LST. LST and NDVI had a negative relationship and were stronger in green

coverage areas compared to built-up areas. At a sub-region level, a higher rise in LST and tremendous vegetation loss were found at high altitudes in the Central Mountain Range, which is located in the southern regions. At the pixel level, urbanization and agricultural expansion had caused increasing LST, while afforestation had contributed to cooling. The study also indicated that the diverse pattern of LC variation has a significant influence on daytime LST, but not on nighttime LST trends. There was an affected of daytime and nighttime LSTs at an altitude above 600 m. However, the growth rates of greenness have not yet decreased, policymakers and practitioners have to consider and plan a balanced view of green cities to retain pace with the accelerating surface temperature conditions.

Acknowledgments

I would like to acknowledge my advisor, Assoc. Prof. Dr. Apiradee Lim, and co-advisors, Emeritus Prof. Dr. Don McNeil for their guidance, continuous encouragement support and motivation throughout the completion of this thesis. Moreover, I would like to thank Dr. Noppachi Wongsai and Assit. Prof. Dr. Sangdao Wongsai from Thammasat University for their guidance and valuable knowledge. I am also thankful to all the lecturers, Ph.D. and Master's students for their direct and indirect support during my study and the faculty staff helped me to move forward.

Furthermore, I am thankful to the Faculty of Science and Technology, Department of Mathematics and Computer Science, for facilitating me with a valuable platform in my academic career. Lastly, I am thankful to The Royal Golden Jubilee Ph.D. Program Scholarship under Thailand Science Research and the Innovation (TSRI) and National Research Council of Thailand (NRCT), (Grant No. PHD/0205/2560) for giving me the opportunity to pursue my Ph.D. degree.

Sahidan Abdulmana

Table of Contents

Table of figures

List of table

List of the Abbreviations

MODIS	Moderate Resolution Imaging Spectroradiometer
NASA	National Aeronautics and Space Administration
IGBP	International Geosphere-Biosphere Programme
LST	Land Surface Temperature
NDVI	Normalized Difference Vegetation Index
LC	Land Cover
LU	Land Use
CI	Confident Interval
QC	Quality Control

Chapter 1

Introduction

1.1 Background and Rational

Land Surface Temperature (LST) is the ground temperature of the earth's surface resulting from land surface-atmosphere reflections and energy fluxes between the surface and the atmosphere (Khandelwal *et al*., 2018). It is a tool for investigating climate change in the heat of the ground surface. One of the significant benefits of LST is that it can be used to monitor rural and global climate change in order to understand environmental situations to sustain human life. However, the transformation of the land surface depends on many aspects for instant vegetation (Kumar *et al.,* 2012), land cover (LC) (Guo *et al*., 2012), and elevation (Phan *et al*., 2018). Normalized Difference Vegetation Index (NDVI) is one of the factors that has been influencing energy balances of the earth surface and affect to LST change (Liu *et al*., 2015). The alterations of vegetation on the ground from short to long term influence climate change at the local to the universal (Bounoua *et al*., 2000). According to Feehan *et al*. (2009) reported that the vegetation trends had reduced in different parts of the world and had a negative association with temperature. In addition, the change in LST and atmosphere were influenced by the vegetation index.

LC is another important factor affecting the changes in LST (Aboelnour and Engel 2018). It is the physical material that makes up the earth's surface. It gives information for the researchers to observe the difference in colors to identify LC in each region. The change of LC is one of the obviously seen influences on the reformation of natural ecosystems from human activities, and it affects the environment from regional to global (Guo *et al*., 2012).

Elevation is the height above or below a fixed geographic reference point, known as a geoid. It is one of the factors that affects climate change. Elevations of 150 meters or below are the places where most of the world's people live (National Geography, 2019). Some of the studies examined the direct influence of elevation on LST from MODIS data and they found that elevation had been shown to have a significant effect on LST, especially in large regions (Phan *et al*., 2018).

Several studies had applied different statistical modeling to find LST patterns. Wanishsakpong and McNeil (2016) reduced spatial correlation by using factor analysis and applied the polynomial regression model of 6^{th} order to predict the pattern of LST. However, the polynomial regression order mainly depends on the use of data and the period. The natural cubic spline model was applied to investigate LST seasonal patterns in Phuket Island, Thailand by Wongsai *et al*. (2017). Nevertheless, global temperature issues are dynamic and difficult to control its undesirable consequences. According to Lean and Rind (2009), they had predicted that the surface temperature around the globe from 2009 to 2019 has been influenced by human activities and that the global surface temperature has been continuously increased.

The characteristics of the land surface have a durable heterogeneity, such as in land cover (LC), land use (LU), vegetation, topography, and soil (Liu *et al*., 2006; Neteler, 2010). In the matter of LU growth and LC transformation, were massive alteration indicated considerable losses in vegetation diversity, ecosystem functions, changes in microclimatic conditions and animals (Dislich *et al*., 2016). Furthermore, natural disasters might transform the LST pattern, for instance, from forest fires, rainfall, earthquakes, and landslides. Tan, (2007) demonstrated that the expansion of cultivation land increases and the vegetation growth cycle affects the surface temperature, which indicates rice paddies absorb heat from their adjacent areas and influence the cooling. Therefore, the measurements require spatially detailed and temporal sampling. Surface assessment cannot essentially provide values over large regions due to the complexity of surface temperature over ground.

In those situations, the advanced technology of remote sensing from satellite data provides the possibility of computing LST over the globe with an adequate and high temporal resolution. To study those alterations, one of the accessible and more reliable sources of LST is from satellite data. The moderate Resolution Imaging Spectroradiometer (MODIS) is a key tool of the National Aeronautics and Space Administration (NASA) that is aboard the Terra and Aqua satellites. In this study, we used data from the MODIS website. There are two satellites installed on MODIS sensors, which are the Terra and Aqua satellites. Those satellites record night-time and day-time for a particular location within a 24-hour period. Daytime and nighttime data from 2000-2020 were included in this study.

From the western Pacific, Taiwan is a mountainous island located in the tropic of cancer and circles on the earth at which the sun can be directly overhead. In addition, the heat in summer has affected on worker health in Taiwan. The highest peak in the Backbone Mountains or the Central Ridge of this island is 3,952 meters. There are two types of monsoon that influence the climate in Taiwan, the summer monsoon from the south-western direction and the winter monsoon from the north-eastern direction (Huang and Hsieh 1994−2003). In addition, the northern part has a heavy manufacturing industries, such as the petrochemical industry. Conversely, the southern region is where the agricultural area for instance, vegetables, fruit, and rice paddy. In addition, there were construction projects ongoing, such as new high-rise apartments, commercial centers and underground transportation systems and the largest population growth at those areas (Ro-Ting and Chang-Chuan, 2009). However, those factors might have an effect on LST in the future. The transformation of vegetation, LC, and elevation might affect LST in Taiwan. As a result, the objectives of our study are to investigate the variations of LST and NDVI across diverse LC types in Taiwan regarding to annual seasonal patterns, decadal trends, their correlations, and dynamic acceleration patterns and to examine the influence of LC variation and elevation on a decadal trend of LST using weighted sum contrasts linear regression.

1.2 Research objectives

5.1 To investigate the changes in LST and NDVI across diverse LC types in regarding to annual seasonal patterns, decadal trends, their correlations, and dynamic acceleration patterns

5.2 To examine the influence of LC variation and elevation on a decadal trend of LST using weighted sum contrasts linear regression that adjusting for each determinate factor

1.3 Expected advantages

1.3.1 The results from this study are useful for Taiwan to understand the temperature change patterns, trends, vegetation index, LC, and elevation which can be useful for developing further plans and policies.

1.3.2 The method used in this analysis can be applied to other comparable time series datasets and is useful for developing a climate change model for other variables such as rainfall, snow, pollutants, air temperature and fire.

1.4 Literature review

1.4.1 Remote sensing

LST shows a significant role in demonstrating meteorological processes, agricultural, ecological and hydrological on the ground's surface. In order to retrieve the spatial distribution of LST can be acquired from thermal remote sensing data by assessing over the ground surface below clear-sky conditions on the upward long wave radiation. Remote sensing uses sensor platforms to detect electromagnetic radiation (EMR) with an essential condition. For measuring the wavelength of LST, thermal infrared (TIR) is used in between 8 and 15 μm. In addition, sensors of satellite TIR obtain EMR that be able to quantify in measuring of Top of Atmosphere (TOA) radiances. This comprises upwelling radiance from the atmosphere, upwelling radiance released from the surface, and the downwelling radiance released by the atmosphere and reflected from the surface.

Some studies used the MODIS satellite sensor to predict and forecast LST change. The Aqua and Terra satellites of NASA support on MODIS which have near polar orbits consequent per day in two images per satellite. Retrieving images on Terra is ∼1030 and 2230 h and Aqua is ∼1330 and 0130 h, all in local time. Those images had a spatial resolution of about 1 km and a high temporal resolution. The products frequently used in LST contain MOD11A1 (Terra) and MYD11A1 (Aqua) which are daily LST and emissivity every 1 km. The advatage of the MODIS sensor is to reconcile among regular image acquisition and suitable spatial resolution compare to another sensors that provide better and resonable spatial resolution. However, with minor temporal resolution (Landsat), or higher temporal resolution but, lower spatial resolution (SEVIRI) (Charlie *et al*., 2011).

The MODIS LST data were used in various studies within the rural climatology fields. In Europe, Pongr´acz *et al*. (2010) explored the Urban Heat Island (UHI) of nine central European cities and found the most intense UHI occurred during the daytime in the summer. According to Hung *et al*. (2006) globally, the UHI quantified in eight Asian mega-cities using MODIS data. Similarly, Jin *et al*. (2005) analysed numerous cities including Beijing and New York, as well as Imhoff *et al*. (2010) used MODIS data averaged over 3 years to calculate UHIs across the United States. In a local study of the Carnarvon Basin in Western Australia, Beardsmore (2005) the estimated LST at specific points across continent extrapolated from borehole thermal gradients temperature was 6 °C warmer than the annual mean air temperature, which is twice the average.

1.4.2 LST and NDVI

The Normalized Difference Vegetation Index (NDVI) is a greenness land of plant health index which are able to investigate the density of flora and plant on the land surface. Vegetation is one of the significant energy balances from the regional to the universal. Furthermore, it takes in carbon-dioxide during the day and releases oxygen to the ecosystem and human beings. In order to explore the alteration of vegetation, scientists have to notice the different colors of wavelengths from visible and near infrared that the floras reflect sunlight. In the area with more leaves, they are reflected more wavelength of light (Przyborski, 2019).

Vegetation can efficiently affect LST by selecting, absorbing and reflecting solar radiation energy for regulating latent and sensible heat exchange (Yuan, 2017). Moreover, NDVI is a plant indicator that is commonly used to assess the association between LST and vegetation (Smith and Choudhury, 1990; Julien *et al.*, 2006). Since, the association between NDVI and LST is influenced by various factors (Ghobadi *et al*., 2014; Qu *et al*., 2014), it is essential to discover the relationship between them. The meta analysis of vegetation was carried out using moderate resolution NDVI and high resolution ground sensor data, as well as the data type (Chandola et al., 2010). In Hungary, Multi-Channel Surface Temperature (MCST) was used to detect the correlation between temperature and vegetation in Hungary (Vadaz, 1994). LST and NDVI (Karnieli *et al*., 2010), advanced very high resolution radiometer (AVHRR) (Vadasz, 1994), and surface air temperature (Johannessen *et al*., 2004) were among the variables commonly used to find out the changes in respective trends.

1.4.3 LST and LC

LST is used to investigate land surface change, surface energy balance, and surface physical and chemical processes. It is extensively applied in biology, hydrology, geochemistry, and soil (Tomlinson *et al*., 2011; Hoa *et al*., 2016). LC change is a significant factor that affects LST. The surface reflectance and roughness in LU types are incompatible, which leads to dissimilarities in LST (Hou *et al*., 2010). Furthermore, based on urbanization, human activities intend to enhance and the ground cover is quickly transformed (Li *et al*., 2017). As a result, the association between LST and LU should be examined to further analyse the ecological effects of LST in addressing national environmental problems.

Currently, many researchers have applied remote sensing to analyse the correlation between LST, LU, and NDVI (Stroppiana *et al*., 2014; Wen *et al*., 2017). However, there is a problem and a limitation to be handled. There were different study methods have been applied, for instance, directly using brightness temperature (Cai *et al*., 2011), which have been used to investigate LST, resulting in decreasing data accuracy. Furthermore, many studies focused on big cities, such as Tokyo (Shigeto, 1994), Shanghai (Yue *et al*., 2006), Bangkok (Estoque *et al*., 2017), and it might be the effect of urbanization which related to land transforms and urban heat island influence in these cities on LST (Pan, 2016). Yuanhong *et al*. (2018) showed that construction of LST on the ground and the standard deviation were the highest. Generally, the construction of land surface, cultivated land, and unused land, that had the highest intensity of human activity. On the other hand, the surface temperature of grassland, forest land, and water bodies, which had the lowest intensity of human activity. However, LU types would be reasonably planned and a cooling influence would be encouraged through water and green vegetation.

1.4.4 Elevation

The elevation term is generally used when referring to points on the ground surface. It is the height above or below a fixed geographic reference point, known as geoid and is one of the significant factors that influence ground surface temperature change. Most of the world’s people live in areas at elevations of 150 meters or below (National Geography, 2019). There were a few number of previous studies have investigated the influence of elevation variation over LST. According to Khandelwal *et al.* (2018), they reported that there was a high correlation between LST and elevation in the surrounding Jaipur area of India in most seasons at nighttime MODIS Aqua LST. Furthermore, the decreasing trend of surface temperature is found in high elevation which is consistent with the study conducted by Pepin *et al.* (2019). They reported a warming rate decline at very high elevations in the Himalaya across the Tibetan Plateau. In addition, other previous studies have examined the direct influence of elevation on LST from MODIS data at both daytime and nighttime and found that elevation significantly affected LST across large areas in northwest Vietnam. Furthermore, the association of both variables was stronger for the nighttime compared to the daytime. (Phan *et al.*, 2018).

1.4.5 Statistical methods

With the help of statistical methods and models applied, LST, vegetation changes, LC, LU, and elevation can be measured. There is a difference between the methods used in the previous studies depending on the data types and their management. According to Johannessen *et al*. (2004), they used a computer simulation of ECHAM4 and HadCM3 models to determine the alterations of arctic climate by combining surface air temperature and sea ice. They applied these models in order to analyse relevant multidecadal to century datasets. Moreover, it is a modern method to investigate an intercomparison of climate change scenarios. From 1892 to 1999, at the Northern Hemisphere altitudes, the empirical orthogonal functions were applied to analyse the influence of climate change on surface air temperature (Semenov, 2007).

In determining the intra-annual global vegetation change, a piecewise logistic model was applied to the Northeastern side of the USA (Zhang *et al*., 2003). This model allowed for the monitoring of vegetation dynamics at large scales and did not require the use of user-defined criteria or pre-smoothing of data. Furthermore, there was effectively assessed the reflectance of canopy biomass vegetation by using the least square linear regression method in Denmark (Hansen and Schjoerring, 2003). This model used data compression by decreasing a large number of measured collinear spectral variables to a few non-correlated principal components.

Multiple linear regression model was applied in the meta-analysis to explore a correlation between LST and NDVI. This method is used to classify which climatic factors are most strongly correlated to the spatial distributions of the dependent variables in different seasons. It shows that they were negatively associated between LST and NDVI at the middle of the growing season (karnieli *et al*., 2010). Although, in the North Atlantic Ocean, linear regression model was used to adjust the spacial seasonality of sea surface temperature (SST). Factor analysis was applied for examining patterns and trends of SST and a multivariate linear regression model was applied for account the spatial correlations between adjacent grid boxes (McNeil and Chooprateep, 2014). They discovered that SST had risen at a rate of about 0.13 °C per decade.

In addition, the linear regression model was applied to illustrate the daily maximum temperatures adjusted for seasonality. This method is applied to model the trends but might not be the better model to estimate trends for shorter periods. Furthermore, factor analysis was applied to categorize the temperatures into seven factors from the 85 stations that correspond to seven geographical regions in Australia

(McNeil and Wanishsakpong, 2012). They found that every region indicated different periodic changes and these were examined using a 6^{th} order polynomial regression model which showed geographic regions had similar temperature patterns. However, they suggested this model is not appropriate for forecasting trends and there is no definite proof that the trends can be forecasted. Furthermore, Wongsai *et al*. (2017) used the cubic spline function and weighted least square (WLS) regression to model the seasonal pattern of annual LST without evaluating missing values. The result illustrated that the seasonal pattern was the same every year. They concluded that by using the cubic spline function, they pleasingly modeled the seasonal pattern, although when there were various missing values in the data sets. In addition, it efficiently modeled the LST of MODIS data that was affected by spatial autocorrelation and can be applied to other time series coverage areas.

1.5 Scope of the Research

This study focused on the modeling the annual seasonal patterns, decadal trends, correlation, and dynamic acceleration patterns changes of LST and NDVI across diverse LC types and to examine the influence of LC variation and elevation over the last 20 years of LST by using linear regression to adjust for each determinate factor in Taiwan from 2000 to 2020. The data were retrieved from the MODIS-Terra satellite. The cubic spline function is a method for smoothing the spline curve and for illustrating the seasonal patterns and decadal trends. Furthermore, to automatically adjust spatial correlation, it used a multivariate regression model in order to estimate decadal trends of LST increase or decrease in each sub-region and region. Lastly, the weighted sum contrasts linear regression was applied to compare the mean of all the interested factors to assess their effect on the LST trends. All statistical analyses and appropriate plots were implemented using the R program (R Core Team, 2020).

1.6 Conceptual framework

The figure 1.1 below is the conceptual framework of the study in order to illustrate the methodological steps of the analysis.

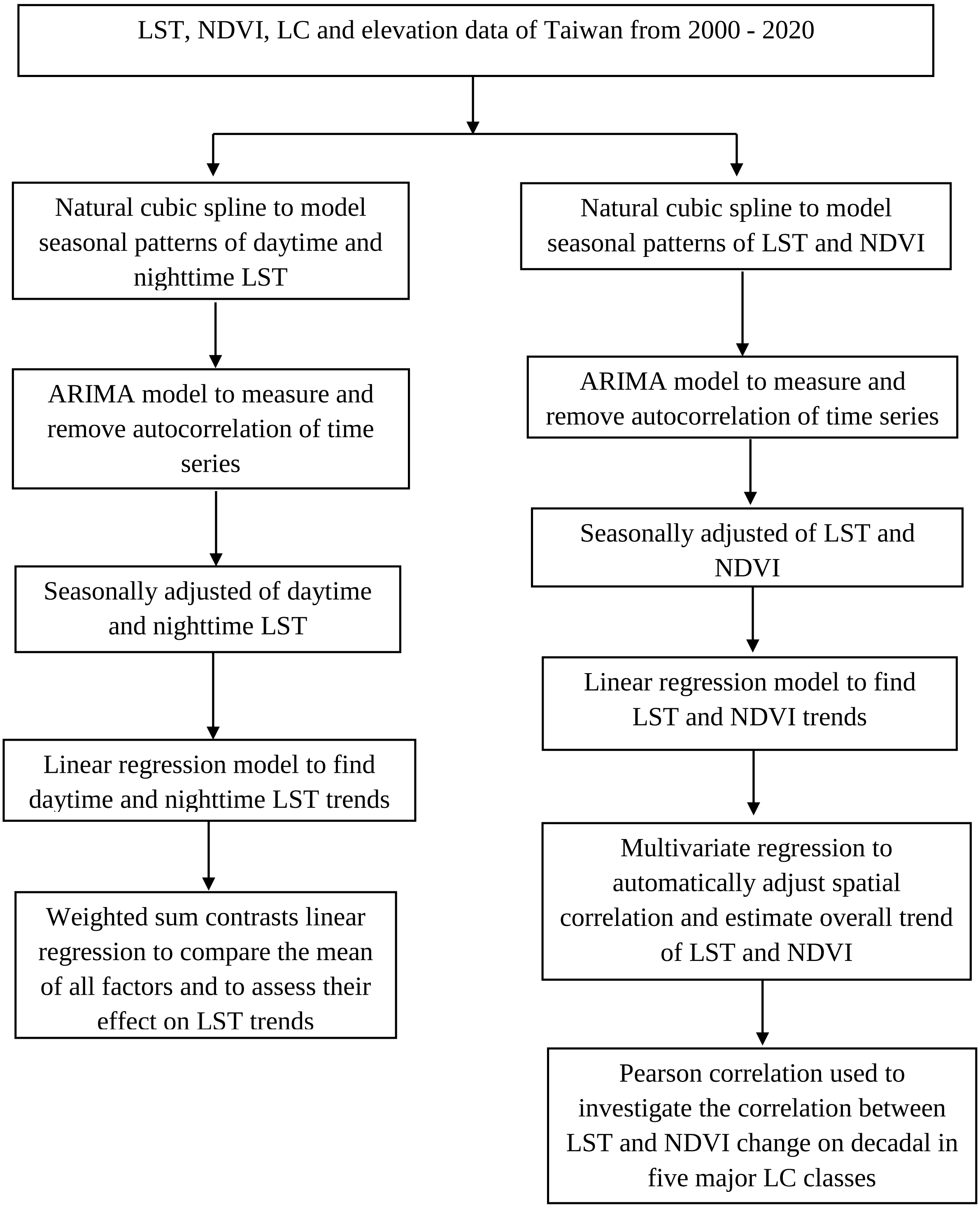

Figure 1.1 Data analysis diagram

1.7 Organization of the thesis

This thesis comprises of four chapters and their details are described below:

Chapter 1 represents the background and rational, research objectives, expected advantages, literature review, scope of the research, conceptual framework, and organization of the thesis.

Chapter 2 represents the description of the method used includes area of study, data use, and the methods use.

Chapter 3 describes the results that model the seasonal patterns and trends from cubic spline, linear regression, and multivariate regression, and Pearson correlation.

Chapter 4 presents the discussion and conclusion of the research findings together with limitations and recommendations for further study.

Chapter 2

Methodology

This chapter describes the methodology used to manage and analyze the data in this analysis. It explains the area of the study, data used, data management, and statistical methods to complete this study.

2.1 Study area

Taiwan was selected as the study area. Furthermore, Taiwan island is distinguished by its distinct eastern two-thirds. It contains rugged mountains running in five ranges from the southern to the northern tip of the island. The Taiwan island has an area of 35,883 km^2 (Figure 2.1). Taiwan consists of 23 cities which are Yujing, Lugu, Zhongxing New Village, Hengchun, Jincheng, Donggang, Magong, Puli Daxi, Yilan, Douliu, Nantou, Yuanlin, Hualien City, Keelung, Taoyuan City, Hsinchu, Banqiao, Kaohsiung, Taichung, Taitung City, Tainan and Taipei (World Population Review, 2018). The study area covered the whole Taiwan island.

The climate of Taiwan is similar to Hainan, Guangxi, and Guangdong provinces in the south of China. Throughout the year, the average temperature in Taiwan is 22°C. In winter, there is no extremely cold but in the summer weather is extremely hot and of high humidity. In the northern part, the annual average temperature is approximately 21.7°C whereas in the southern part is approximately 24.1°C. The coolest months are January to March, with low temperatures of around 10°C. In some unusual situations on the high mountains, there will be snow or frost. From June to August are the hottest months with the highest temperature up to around 38°C. From the rest months, the average temperature is approximately 25°C.

In this study, 1×1 km^2 LST, 250×250 m^2 NDVI pixels, LC, and 250 m elevation sited only on Taiwan Island were used. LST data were downloaded into eight super-regions which cover the area of 50×50 km^2. Then, Taiwan was separated into 21 sub-regions for regional and overall trends analysis of LST and NDVI using QGIS software, as demonstrated in Figure 2.1 (a). Figure 2.1 (b) presents the MODIS LC types of Taiwan, categorized best on the International Geosphere-Biosphere Programme (IGBP). There is subtropical climate of Taiwan island, excluding for the southern part of the Taiwan, which is tropical. The Taiwan season consists of two different seasons with mild winters, rainy summers and hot. From December to March are the shot winters. In the north, at lower elevations, there was snowfall in the mountains and the occasional ski resort. Summers on the east side of the island and in the mountains, which are most affected by stronger typhoons and a lot of rain between April or May to September or October.

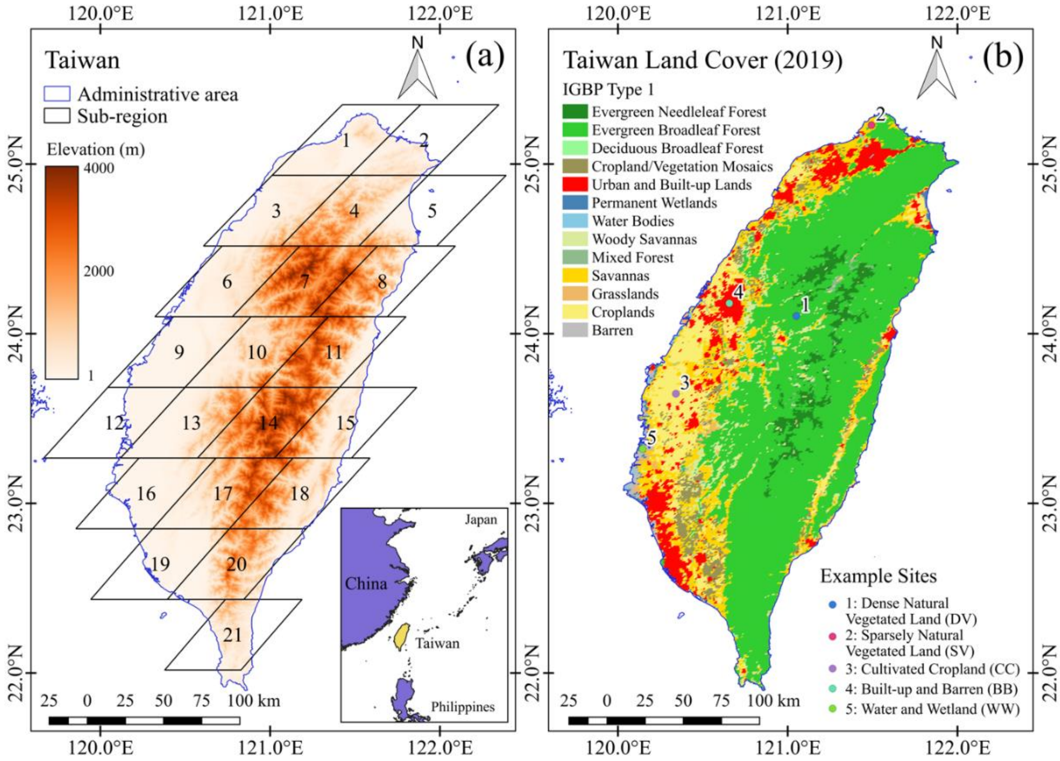

Figure 2.1 The map of (a) Taiwan representing elevation and 21 sub-regions, and (b) IGBP LC types over Taiwan island with five example sites. Note that land cover class legends display only classes found in the study area.

2.2 Data used

2.2.1 LST data

LST (MOD11A2) was ordered from the MODIS Land Product subset tool (ORNL DAAC, 2018). LST data was obtained from February 18, 2000 to February 11, 2020, which is approximately 20 years of data observation. The MOD11A2 product is a level 3 MODIS/Terra LST and Emissivity at 8-day temporal with 1 km spatial resolution (Wan and Hulley, 2015). Therefore, there are 46 observations in each year, and 920 observations for the total number over the last 20 years.

The acquitted LST data cover daytime and nighttime LST data (around 10:00 and 22:00 at a local solar time). Moreover, it includes the quality control data (QC_day and QC_night) layers for an extra data on the LST quality generation due to other data conditions. Therefore, this study used both the daytime and nighttime LST datasets that cover Taiwan island (41,784 pixels in total) meanwhile LST at the nighttime does not adjust over LC types. This study omitted the quality control data because the results were not a significant different. When conducting the method testing, the QC day layers were initially used. We specified the weighed matrix according to the average LST error provided in the layer of QC_day where the error of LST <= 1K is allocated as 10, then for LST error <= 2K is assigned as 5, then for LST error <= 3 is assigned as 3, and for LST error > 3 is assigned as 1 (Wongsai *et al*., 2020b). Then, a weighted sum contrast linear regression method was fitted on each LST series from 5 example sites (with diverse LCs). The finding have no significant difference compared to fitting a simple linear regression model since there was a minor alteration of QC in the last two decades of LST data in the area of study. Therefore, we considered not to apply QC data in this analysis because of the simplicity of the data analysis and computation efficacy.

2.2.2 NDVI data

NDVI data (MOD13Q1) product was retrieved from the MODIS Land Product subset tool (ORNL DAAC, 2018). NDVI data was obtained from February 18, 2000 to February 11, 2020, which is approximately 20 years of data observation. In addition, the spatial resolution of vegetation data from the MOD13Q1 product is 250 m at 16-day temporal and level 3 MODIS/Terra Vegetation Indices (VI). Consequently, there are 23 observations per year, adding up to 460 observations of NDVI time series in the 20-year.

2.2.3 LC data

MODIS Land Product subset tool (ORNL DAAC, 2018), it includes land cover (LC) type of the year 2019 data (MQD12Q1) in comma-separated value (.CSV) file format. IGPB Type 1 LC types were provided by the MQD12Q1 product with a spatial resolution of an original 500 m. In order to match with the MOD11A2 LST product of a 1 km spatial resolution, we downloaded the LC data from the MODIS Land Product subset website. There were 13 LC types out of 17 types of LC as stated by the IGBP classification were established in the area of study. To evaluate the last two decades relationship among LST and NDVI trends in regions of different LCs, we rearranged 13 LC types into five main groups, as shown in Table 2.1. New groups of LC type comprised 1.5% of Water and Wetland (WW), 9.4% of Built-up and Barren (BB), 16% of Cultivated Cropland (CC), 14.2% of Sparsely Natural Vegetated Land (SV), and 58.9% of Dense Natural Vegetated Land (DV). For illustration in this study, one example site was chosen from each of these five main LC groups (Figure 2.1b).

Table 2.1 IGBP LC type, LC group and its coverage percentage in Taiwan, 2019

<table>
<tr><th rowspan="2">Group Name</th><th colspan="2">IGBP Land Cover Type</th><th rowspan="2" colspan="2">% coverage</th></tr>
<tr><th>No.</th><th>Class Name</th></tr>
<tr><td rowspan="4">Dense Natural Vegetated Land (DV)</td><td>1</td><td>Evergreen Needleleaf Forest</td><td>3.7</td><td rowspan="4">58.9</td></tr>
<tr><td>2</td><td>Evergreen Broadleaf Forest</td><td>54.3</td></tr>
<tr><td>4</td><td>Deciduous Broadleaf Forest</td><td>0.1</td></tr>
<tr><td>5</td><td>Mixed Forest</td><td>0.8</td></tr>
<tr><td rowspan="3">Sparsely Natural Vegetated Land (SV)</td><td>8</td><td>Woody Savanna</td><td>5.9</td><td rowspan="3">14.2</td></tr>
<tr><td>9</td><td>Savanna</td><td>6.8</td></tr>
<tr><td>10</td><td>Grassland</td><td>1.5</td></tr>
</table>

Cultivated Cropland (CC)	12	Cropland	10.6	16.0
	14	Cropland/Natural Vegetation Mosaics	5.4	
Built-up and Barren (BB)	13	Urban and Built-Up	9.0	9.4
	16	Barren	0.4	
Water and Wetland (WW)	11	Permanent Wetland	0.9	1.5
	17	Water Bodies	0.6	

2.2.4 Elevation data

The Global Multi-resolution Terrain Elevation Data 2010 (GMTED2010) data set was used in this study (Danielson and Gesch, 2011). Raster elevation data with 7.5-arc-second spatial resolutions (250 m) were downloaded from the United States Geological Survey (USGS) Earth Explorer website. The GMTED2010 product comprises seven sets of elevation data for each of the 30-, 15-, and 7.5-arc-second spatial resolutions. However, the 30-arc-second resolution (1 km) product was not exactly matched with 1×1 km^2 pixels of the obtained MODIS LST and LC products. Thus, we used 7.5-arc-second spatial resolution (250 m) median elevation dataset. We grouped elevation into nine levels, as detailed in Table 2.2, to investigate the effect of elevation on the change of LST in the 20-year period of study.

Table 2.2 Group of elevation and percentages of pixels for each group

Group	**Distance above sea level (m)**	**% coverage**
1	0 – 49	21.05
2	50 – 99	7.03
3	100 – 179	7.54
4	180 – 349	10.41
5	350 – 599	10.07
6	600 – 999	11.60
7	1,000 – 1,499	11.01
8	1,500 – 1,999	9.24
9	2,000 and above	12.05

2.3 Data management

The original LST data that given from MODIS was in kelvin then, we converted from Kelvin into Celsius by subtract with 273.15 because Celsius is a regular and ordinary scale and unit of assessment for surface temperature. The special resolution of LST was 1 km with emissivity at 8-day temporal. Whereas, a special resolution of NDVI was 250 m with 16-day temporal. Therefore, to match between LST and NDVI values were executed by using QGIS program. Moreover, special resolution of LC types was 500 m. Then, LC data was automatically resampled to match with 1 km special resolution of the LST product by ordering data from the MODIS Land Product subset website. For the special resolutions of elevation was 250 m. However, we used 7.5 arc-second spatial resolutions to aggregate with 1 km LST pixel with median value by using the QGIS program. It used the Zonal statistics function to generate 1 km LST polygons. The data management of each variable is shown in the following figures.

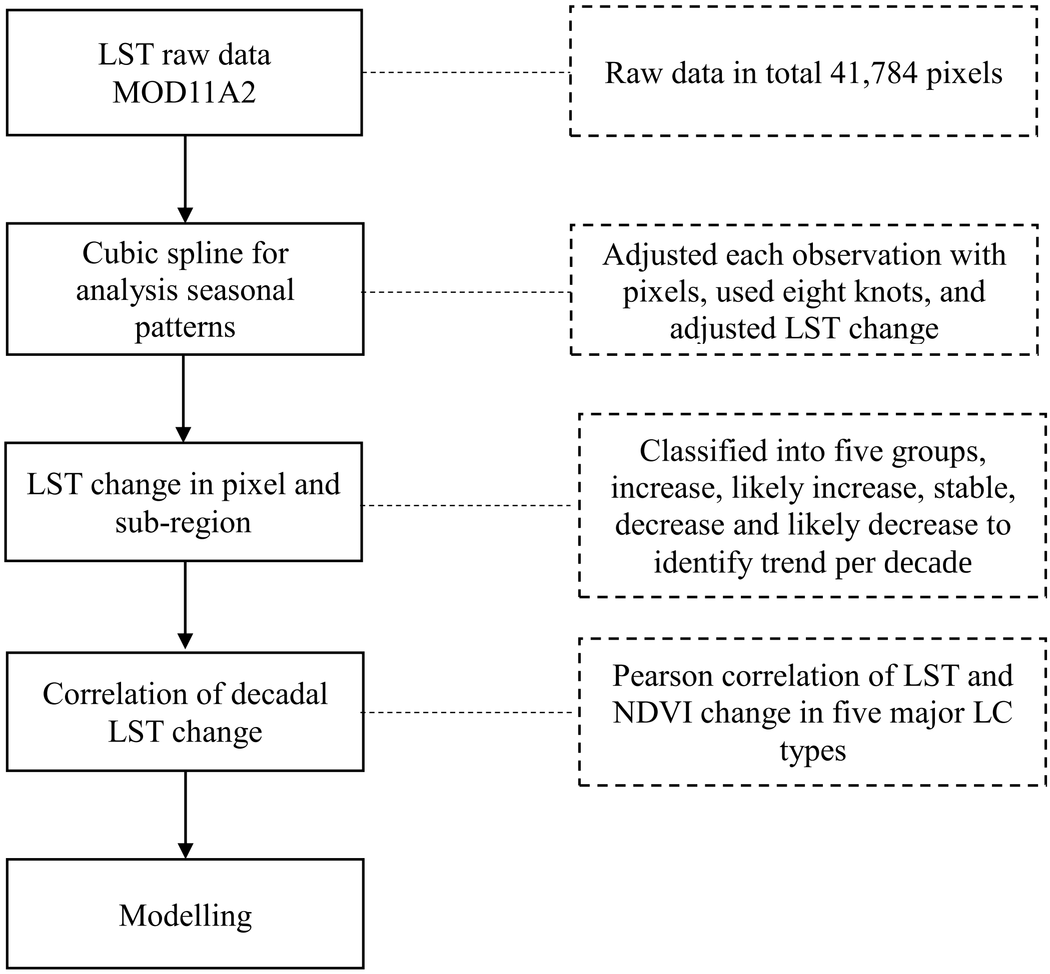

Figure 2.2 Process of managing LST data

Daytime LST data were adjusted to the pixel coordinates latitude and longitude. The eight knots from the cubic spline function were assigned to investigate seasonal patterns. Then, seasonally adjusted time series were calculated by subtracting the original values with fitted values from the natural cubic spline and adding the mean values of each sub-region back to confirm that the average temperatures over the 20 years were not changed. LST changes per decade by pixel and sub-region were fitted with linear regression to estimate the LST trends. Lastly, decadal LST data was used to investigate the relationship between LST and NDVI decadal changes in five major LC types.

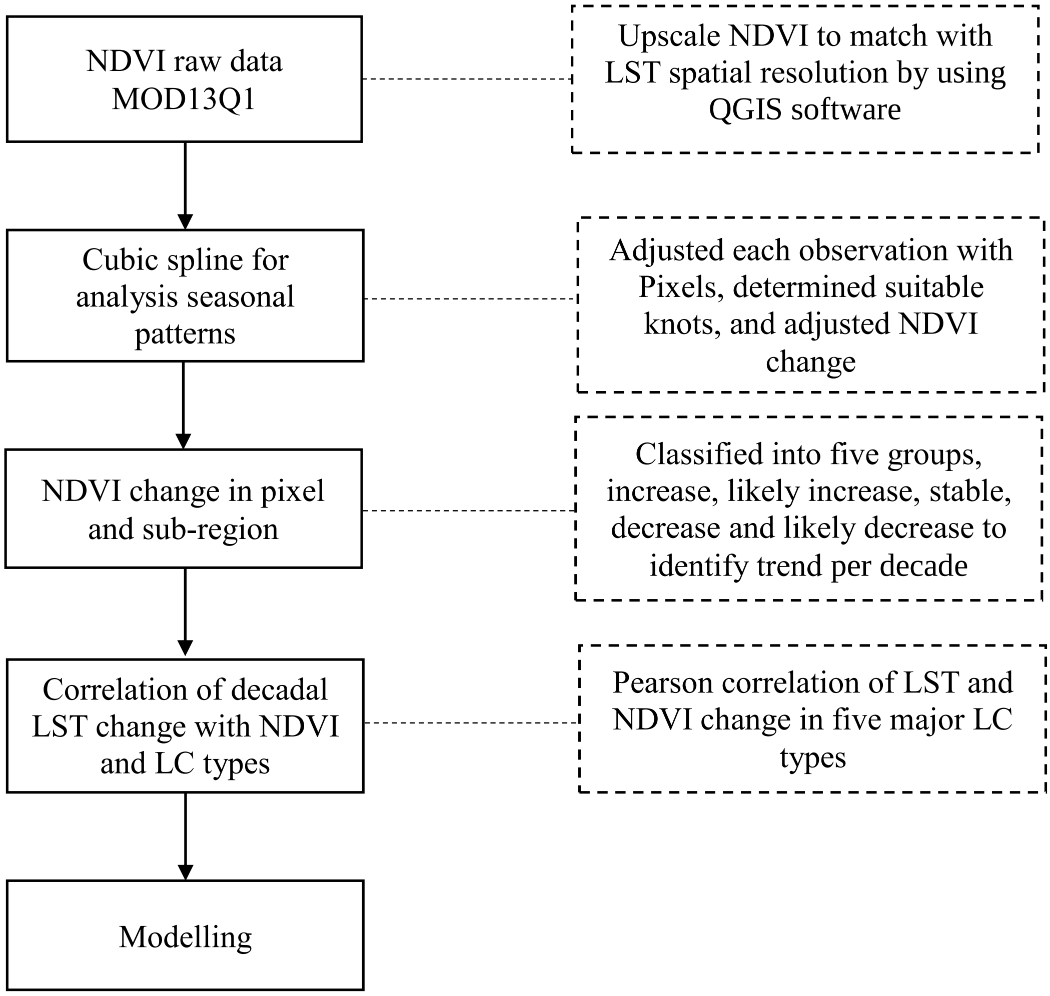

Figure 2.3 Process of managing NDVI data

In managing NDVI data to match with LST pixel, we upscaled NDVI data to math with the spatial resolution of LST by taking an average of 250 m at 16 original values within a 1 km^2 of LST pixel. The performance of matching was done using QGIS program. Initially, we used projection/grid conventional formulas to create LST pixels shapefiles forming polygons and points at the middle of NDVI pixels. Then, these shapefiles were connected to the original LST and NDVI pixel ID from the CSV file. Finally, a mean value of 16 NDVI points located inside a LST polygon was evaluated by using the QGIS Zonal Statistics function.

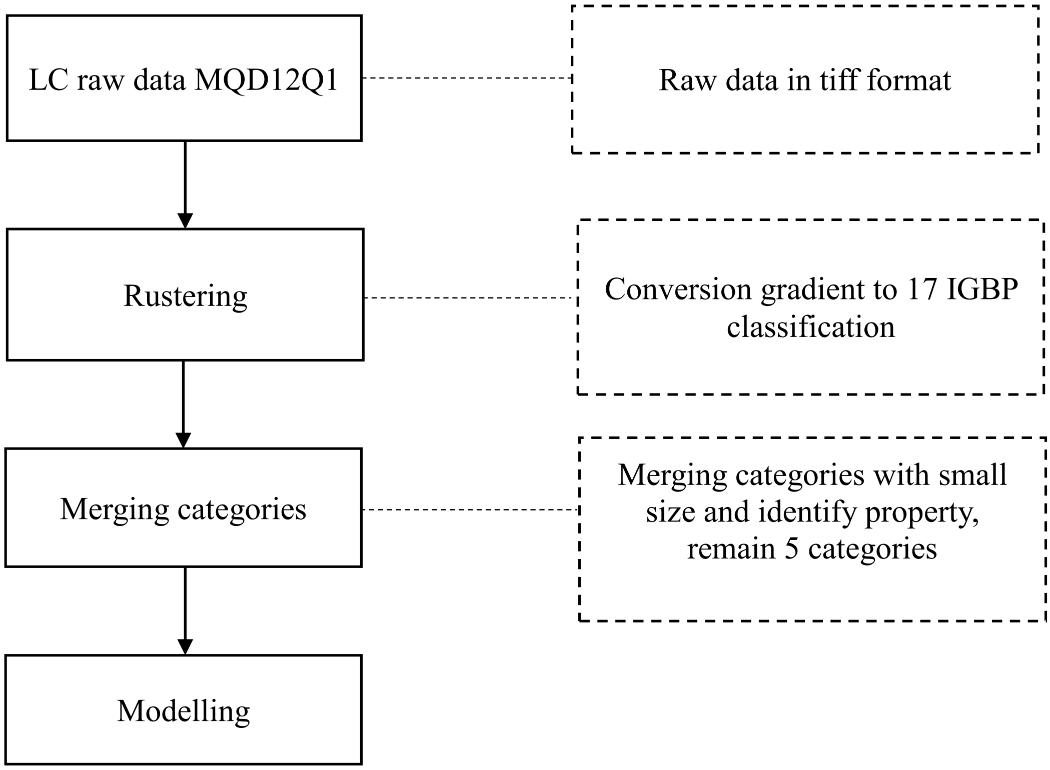

Figure 2.4 Process of managing LC data

LC product of the year 2019 provided IGPB classification types with a spatial resolution 500 m. Then, we resampled to match with 1 km LST spatial resolution by ordering data from MODIS Land Product. LC data were obtained from the MODIS data maps, which were then converted to vectors using QGIS software. To investigate the seasonal patterns and trends of daytime LST and NDVI and their correlation on decadal change we re-grouped from 13 types to five major groups. Furthermore, in order to analyze LC change, we download another LC data set product from 2001 and converted to vectors using QGIS software. Then, we used transition matrix between year 2001 and 2019 to investigate the distribution of LC change. To examine the influence of LC variation on decadal LST trend, we classified into nine classes.

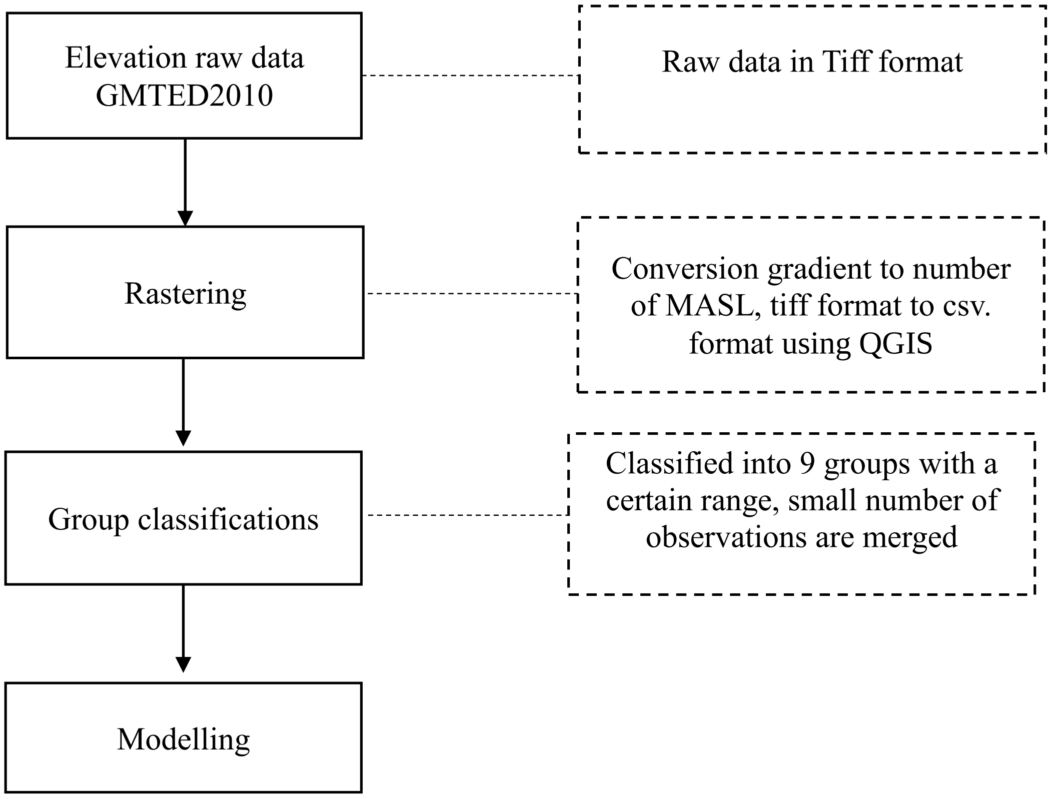

Figure 2.5 Process of managing elevation data

Raster elevation data was provided by the USGE website contains seven sets of elevation data. In this analysis, we used 250 m (7.5-arc-second special resolution) with the median elevation dataset to aggregate with 1 km LST pixel by the median value. QGIS software was used to downscale of elevation using the Zonal Statistics function to generate 1 km LST polygons. There were nine levels as shown in Table 2.2 was grouped to examine the effect of elevation on the change of 20 years of LST.

2.4 Statistical method

A cubic spline is a spline function constructed from a piecewise third order polynomial where the second derivatives of each polynomial are normally set to zero at the endpoint. It provides the smoothest model between all the functions and is usually applied to smooth different types of data in study areas, for example, satellite-based time series data (Mao *et al*., 2017), interactive computer graphics (Smith *et al*., 1994), and real-time digital signal processing (Feng, 1998).

In this analysis, there were eight knots of the cubic spline function allocated at Julian Days 10, 40, 80, 130, 240, 290, 330 and 360 were fit to the data to determine the spline function coefficients. The placement number of the knots was identifid the variation of the data and r-square. Then, a linear regression model was used to evaluate the annual seasonal patterns of the time series by fitting the observation time and the coefficients to the data of outlier-free (Wongsai *et al*., 2017). A linear regression model formula used in this study is

$$y_i = \alpha + \beta_0 x_i + \beta_1 c_{k,i} + \ldots + \beta_p c_{k,i} + \epsilon_i \tag{1}$$

for $i = 1, 2, \ldots, n$. x is the observations day, c_k is the cubic spline function coefficients resulting from knot $k = 1, 2, \ldots, 5$. Then, we allocated eight knots for the cubic spline function with the annual periodic boundary condition, five coefficients were computed and the assigned knots number were subtract with this specified cubic spline free coefficients. The seasonal pattern was obtained from the fitted value of the above regression model. Lastly, seasonally adjusted daytime LST were calculated by subtracting the original values with fitted values from the natural cubic spline and adding the mean values of each sub-region back to confirm that the average temperatures over the last 20 years were not changed.

Even though the use of a linear regression model could depict an actual trend from time series of seasonally adjusted ($T_{s.adj}$), the autocorrelations among errors at two identified time points are supposed to be independent and uniformly disseminated or fixed. The error term of this autocorrelation could influence the standard error of the assessed parameters and requires to be controlled properly when a regression-based analysis model was applied. This is because the goodness of fit is frequently calculated from the residues. In order to eliminate those autocorrelation from the time series, a non-seasonal autoregressive integrated moving average (ARIMA) model was applied. The ARIMA method is normally denoted as ARIMA(*p*,*d*,*q*), where the three non-negative integer components (*p*,*d*,*q*) are the order of the moving-average process, the degree of distinction and the number of time lags (the autoregressive order), correspondingly. In this analysis, ARIMA(*3*,*0*,*0*) model was used to measure the correlation of time series values at two diverse time lags, and their standard error (SE) were explored and compared. Then, ARIMA(*p*,*0*,*0*) model of the fitted residuals with *p* that accounts for the most autocorrelated errors in the time series were chosen and applied to filter the time series. The filtered $T_{s.adj}$ was computed from the following formula:

$$\text{Filtered } \mathrm{T}_{\mathrm{s.adj}} = \left[\left(\frac{\sigma(\mathrm{T}_{\mathrm{s.adj}})}{\sigma(\epsilon)}\right) \times \epsilon\,\right] + \mu(\mathrm{T}_{\mathrm{s.adj}}) \tag{2}$$

where ϵ is the residual that fitted from the selected ARIMA(*p*,0,0) model, σ is the population standard deviation term, and μ is the term of a population mean.

The step explained before was used for each time series of LST and NDVI in order to produce filtered seasonally adjusted LST ($LST_{s.adj}$) and NDVI ($NDVI_{s.adj}$) time series for future analysis.

2.4.1 Seasonally adjusted and time-independent series

The time series of LST and NDVI normally involve seasonal patterns, trends, and noise elements similar to other time series. Seasonality strongly affects an inter-annual LST and NDVI time series data. However, before investigating alterations and correlations over 20 years, seasonal adjusted of LST and NDVI data were required. The annual periodic boundary conditions of the cubic spline function was implemented to model a yearly seasonal pattern that certifies continuity and smoothness of seasonality for LST and NDVI pixels or time series. Wongsai *et al*. (2017) was applied this method for modelling LST time series from MODIS data for long period on Phuket island of Thailand and had been used in another areas involving Peninsular Malaysia (Ismail *et al*., 2019), New Britain Island of Papua New Guinea (Devi *et al*., 2021), Kathmandu Valley, Nepal (Sharma *et al*., 2018a; Sharma *et al*., 2018b), Central Sumatra, Indonesia (Prasetya *et al*., 2020), Spitsbergen Island of Norway (Fitrahanjani *et al*., 2021), and Mainland Southeast Asia (Wongsai *et al*., 2020b).

As a result, abnormally low NDVI values because of cloud contamination from the seasonality extraction process were excluded. Furthermore, irregular temperatures at a specific time of a year, denoted to as extreme LST values that influence by an irregular situation of LC changes such as floods, bushfires, and other natural disasters were also omitted.

2.4.2 Twenty-year LST and NDVI Dynamic analysis

Natural cubic spline function was used to investigate the dynamic of filtered seasonally adjusted LST ($LST_{s.adj}$) and NDVI ($NDVI_{s.adj}$) time series. The function computes from the following formula

$$s(x) = a + bx + \sum_{k=1}^{n-2} c_k\left[(x - t_k)_+^3 - d(x - t_{n-1})_+^3 + e(x - t_n)_+^3\right] \quad (3)$$

where $d = \frac{(t_n - t_k)}{(t_n - t_{n-1})}$, $e = \frac{(t_{n-1} - t_k)}{(t_n - t_{n-1})}$. The time-point of observation within an interval $[a,b] \subset \mathbb{R}$ is indicated as x, and the knots set given as $\{t_k\}_{k=1}^{n}$ if $t_k < t_{k+1}$ for every k = 1, …, n – 1 and both $t_1 \geq a$ and $t_k \leq b$. The term $(x - t_k)_+$ is the derived spline coefficients where $(x - t_k)$ for $x > t_k$ and 0 otherwise. Once again, as denoted in Equation 1, the regression model was used to fit derived coefficients of spline function to the filtered $LST_{s.adj}$ and $NDVI_{s.adj}$. There are two sets of knots were assigned (zero knots and four knots) to evaluate linear and actual forecasting trends. Remind that, in the set of zero knots, the regression model is only the simple linear regression model (shown in equation 1). The independent variable was only the day of observations. Lastly, the regression model fit with zero knot spline coefficients was applied to estimate LST and NDVI (ΔLST and ΔNDVI) changes. The regression fitting of *p*-value was recorded and displayed as a thematic map. The curvature acceleration trend was computed from the spline coefficients of four-knot by using the following formula, which was applied by Wongsai *et al*. (2020a).

$$3 \times c_1(t_3 - t_1) + 3 \times c_2(t_4 - t_2) \times (t_3 - t_2)/(t_4 - t_1) \tag{4}$$

The speedily or slowly increases/decreases in the decade were used as an acceleration rate to describe the temperature variation. Reminder that the extreme LST and NDVI values exceed three times the standard deviation from the means of filtered $LST_{s.adj}$ and $NDVI_{s.adj}$ were excluded from this dynamic and trend analysis to ensure normality of data. An association between the acceleration rates and the linear trends were investigated to recognize the acceleration patterns of the 20-year dynamic of LST and NDVI.

2.4.3 Overall decadal change of LST and NDVI in Sub-region

A linear regression model was fitted to aggregate individual time series within the sub-region. It could encounter significant associations among the residual terms since an observed LST, or NDVI values at a certain pixel are normally associated with nearby or surrounding pixels. The strong spatial autocorrelation possibly influences the assessed parameter and standard error (SE) of the model. To remove spatial correlation and to evaluate the overall trends in the sub-region of LST and NDVI in the entire Taiwan Island, we used multivariate regression model to solve those problems. The formula for multivariate linear regression is shown in the following form:

$$f_{ij} = \alpha_i + \beta x_i + \epsilon_{ij} \tag{5}$$

where $f_{i,j}$ is the filtered $T_{s.adj}$ matrix at observation i in time series j, x_i is an observation time-point with i = 1, 2, …, n (n = 920: observation number in 20-years period), and β is the estimated variation per observed time series where the total of 20-year trends can be calculated from it. Furthermore, the mean of the multivariate outcomes SE, as denoted in formula 5, was calculated subsequently it can fit parameters for dissimilar dependent variables to be compared in such spatial correlation case represented.

$$\mathrm{SE(mean)} = \sqrt{\textstyle\sum_{i,j=1}^{n,p} V_{i,j} / n} \tag{6}$$

where, $V_{i,j}$ is the estimates variance-covariance matrix from the multivariate regression model, p is the number of time series or pixel within the region and n is the observation number. This variance-covariance matrix was delivered for the estimated variation of data, providing confidence intervals (CI) for linear combinations of variation in diverse time series. Reminder that in a multivariate regression model, a missing value at any row in the response matrix is omitted. Consequently, the missing values were filled by using the fitted values from the regression of filtered $T_{s.adj}$. The total values of change and z-score of the overall trends were illustrated as a thematic map. The z-score presented the variation in how many standard deviations from the mean of observed values represent the normalized measurement of LST and NDVI change at 95% CI without the actual unit.

2.4.4 The effect of LC change and elevation on LST

As we used a regression model to evaluate the influence of LC change and elevation on long-term LST data, seasonally adjusted LST ($LST_{s.adj}$) time series needs to account for autocorrelation. Time-dependent in time series data could influence the standard error of the estimated parameter in the regression-based analysis model, which could narrow its confidence intervals, and the statistical assumption of independent and identically distributed error term at two specified time points is violent. To eliminate autocorrelation in $LST_{s.adj}$, a non-seasonal autoregressive integrated moving average (ARIMA) model with a maximum of three lags was used to measure the maximum correlation of time series values between two different time lag (Wongsai *et al.*, 2020a). Then the $LST_{s.adj}$ series were filtered to reduce autocorrelation by using the following formula:

$$\text{Filtered LST}_{\text{s.adj}} = \left[\left(\sigma\left(\text{LST}_{\text{s.adj}}\right)/\sigma(\epsilon)\right) \times \epsilon\,\right] + \mu\left(\text{LST}_{\text{s.adj}}\right) \qquad (7)$$

where "ϵ" is the fitted residual from the designated ARIMA(p,0,0) model, "σ" is the term of population standard deviation, and "μ" is the term of population mean (Wongsai *et al.*, 2020a).

2.4.5 The Weighted Sum Contrasts Linear Regression

In this study, the outcome was the estimated increase/decrease LST in a decade resulting from the linear regression fitting of filtered $LST_{s.adj}$ data series, categories of elevation, and groups of LC change pattern were the determinants of interest. When a determinant in a regression model is a categorical variable, the formula model is formulated as a set of k - 1 parameters, where k is the number of different categories. x_1 is the identity of the elevation group, and x_2 is the identity of the LC change group. Since factor(x_1) only has k - 1 parameters, as well as factor(x_2), the model was formulated as

$$y = a + \sum_{i=2}^{k} b_i x_{1i} + \sum_{i=2}^{k} c_i x_{2i} \quad (8)$$

where b_i and c_i were the coefficients of x_1 and x_2 at identity i, respectively, and b_1 and c_1 = 0 in the case that no *contrast* option was selected when specifying the model. In general, if contrast option is not specified, the parameters are matched with each factor level in alphabetical order, but with the first parameter set to 0. A contrast in linear regression is a linear combination of determinants whose coefficients add up to zero, allowing comparison of different treatments (Casella, 2008). The contrasts for this method are known as “treatment” contrasts because they were originally used in experiments designed to compare one or more treatment groups with a control group, where it makes sense to set the parameter associated with the control group to 0, so that the parameters associated with the treatments are the actual treatment effects. However, we have no control group in our study, and consequently, two categories in our determinants and covariates were omitted.

To achieve the objective of our study in comparing the mean of all interested factors to assess their effect on the LST trend, we used *weighted* sum contrasts developed by Tongkumchum and McNeil, 2009. This method suggests constructing confidence intervals for comparing means that did not include choosing a reference group and thus provides an informative confidence interval for comparing each means with the overall mean. When there is no control group, different contrasts called "sum" contrasts can be used. Sum contrasts constrain parameters associated with each factor level so that each gives a measure of its difference from the overall mean of the outcome. The formulation is similar to that for treatment contrasts, with additional terms (b_1 and c_1), that is,

$$y = a + b_1 x_{1i} + \sum_{i=2}^{k} b_i x_{1i} + c_1 x_{2i} + \sum_{i=2}^{k} c_i x_{2i} \qquad (9)$$

For equal sample sizes, the sums of the sets of coefficients are 0, so $\sum_{i=1}^{k} b_i = 0$ and $\sum_{i=1}^{k} c_i = 0$. But this is not the case in our study, where the sample sizes for the elevation and LC change groups were unequal, as shown in Table 2.2. As a result, with an unequal sample size, the weighted sum contrast method was used to calculate the mean in each factor level.

During the process of fitting linear regression with *weighted* sum contrasts method, overall mean (average of all LST trends), overall r-squared (adjusted r^2 from regression model without contrast option), crude mean (mean of LST trends in each category of factors), adjusted r^2 and *p*-value for each factor were calculated. All of the computed statistical model's parameters were investigated and compared. This method of weighted sum contrasts collaborating with linear and logistic regression had been used in many preceding studies. It used to compare blood lead levels among children in Pattani river, Thailand (Tongkumchum and McNeil, 2009) and investigated HIV mortality by age group and gender in Thailand between 2014 and 2015 (Tulu *et al*., 2020).

Moreover, the "democratic" confidence intervals for each category of factor were computed for assessing the variation in a mean. The confidence intervals from two-sample t-test and analysis of variance (ANOVA) are valid for each sample individually (and use all the information in the data because they use pooled standard deviations), but they are not appropriate for comparing means. For comparing means, we use confidence intervals for the difference between the means, which is the same as the difference between each mean and the overall mean. They are consistent with the *p*-value and are "democratic" because they do not need to select a control group as a basis for comparison. All applicable plots and statistical analyses were computed by using the R program (R Core Team, 2020).

Chapter 3

Results

3.1 Daytime LST and NDVI Annual Seasonal Patterns and Trends Over 20 Years

There were five example sites placed in different LC types, 20 years daytime LST and NDVI annual seasonal patterns and trends are illustrated in Figure 3.1. The red plus symbol (+) of the left column represents the position of the knots and cross symbol (×) represents omitted observations. The seasonal patterns and trends of filtered $NDVI_{s.adj}$ at the right column and filtered $LST_{s.adj}$ at the middle column applying the natural cubic spline model with the zero knot as represent with red dash line and four knots as illustrate with black thick line, separately. There was an increasing trend during the summer of daytime LST and reached the highest point in the midyear before steadily declining in September to March in the rainy season. Such seasonality was investigated yearly across the distinct LC types, exclude for the WW land where the highest LST was found in an alteration period in early April from winter to summer. The DV land had a lower surface temperature than another categories. NDVI shows a roughly unchanged pattern over the year, but its size order shows an increase from WW, CC, SV, to DV. NDVI seasonal pattern was revealed for the BB types where two peaks were noticeable in April when the summer season begins, and in October when a rainy season starts. In addition, a strong annual dynamic of greenness revealed two green-up periods.

Over 20 years period of the study, BB land had an increased LST at a rate of 0.0862 °C per year or 0.862 °C per decade (°C/dec), denoted by a positive coefficient which p-value < 0.001 whereas the CC land had reduced LST rate by 0.327 °C/dec with *p*-value < 0.05. Vegetation index on BB area shows – 0.024 unit/dec and p-value 0.001 and CC area represents 0.056 unit/dec and p-value 0.001 indicated an adverse LST trend, as estimated. Even though the SV land of LST was not statistically changed over the study period while NDVI was noticed to rise by 0.024 unit/dec (*p*-value < 0.001). In other LC types, LST and NDVI had no evidence of changes.

It should be underlined that fitting the data devoid of knots provides a normal linear trend that shows an overall LST and NDVI change over 20 years but improperly captured long-term dynamic LST and NDVI time-series. Then the trend was straightforward to use a cubic spine model with four-knot. It demonstrates the acceleration rate of LST (°C/dec^2) and NDVI (unit/dec^2). Furthermore, it shows the variations in the increasing or decreasing rate in each decade.

The result shows that there was a rising LST trend on the BB land at the acceleration of 0.337 °C/dec^2 (*p*-value < 0.001) over 20 years. It indicated that LST rises within the first decade and continually increased in the latter decade. There was a similar trend observed in other LC types. During the first decade, the LST trend was declining and then gradually rising subsequently. Nevertheless, there were no statistically significant acceleration rates. The result from the NDVI appears to be constant up to the year 2010 and it persuades to rise toward the end of the period of study. There was a significant increase in the acceleration rate for DV, SV, and CC which were 0.047, 0.044, and 0.060 unit/dec^2 with *p*-value < 0.001, respectively. A reverse trend appeared in the BB area with the declined acceleration rate of 0.002 unit/dec^2 (*p*-value < 0.001).

In subsequent sections, the cubic spline model was extended to fit with the 20-years daytime LST and NDVI time series on the five example sites to cover the entire

Taiwan area for investigating temporal and spatial variations in LST and NDVI patterns and trends.

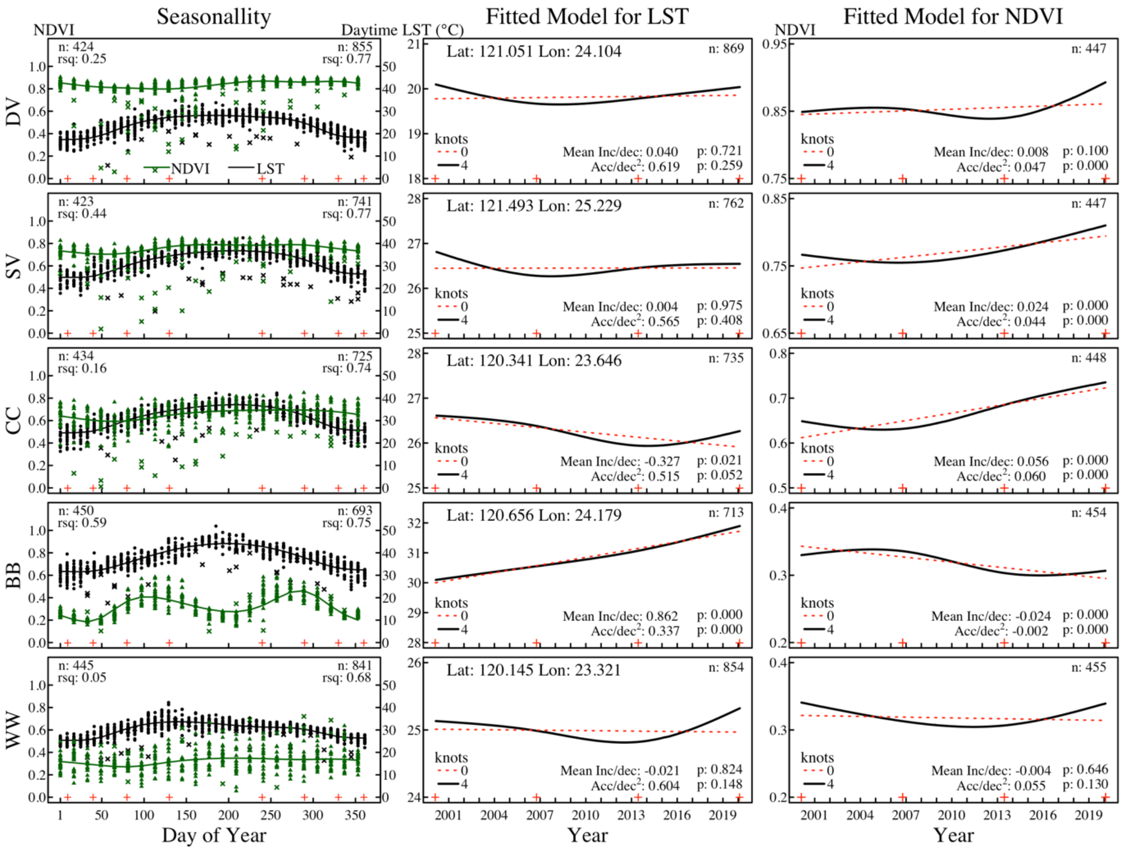

Figure 3.1 Seasonal patterns of daytime LST and NDVI for examples of five LC types

3.2 Decadal Change in Daytime LST and NDVI

Table 3.1: Daytime LST and NDVI increase with 95% CI (Confident Interval) and z-values of each sub-region from 2000 – 2020

Variables	**LST**			**NDVI**		
Sub-Region	**Increase**	**95% CI**	**z-value**	**Increase**	**95% CI**	**z-value**
1	0.143	-0.035-0.321	1.572	0.023	0.017-0.028	7.607
2	0.162	0.007-0.317	2.046	0.036	0.024-0.047	6.051
3	0.024	-0.149-0.198	0.275	0.025	0.02-0.031	9.184
4	0.085	-0.073-0.243	1.055	0.027	0.018-0.035	6.185
5	0.229	0.078-0.381	2.967	0.025	0.016-0.033	5.631
6	0.165	-0.007-0.338	1.875	0.016	0.012-0.021	7.237
7	0.038	-0.133-0.209	0.434	0.028	0.022-0.035	8.428
8	0.075	-0.084-0.234	0.924	0.023	0.014-0.032	4.93
9	0.265	0.084-0.447	2.867	0.013	0.009-0.016	6.282
10	-0.003	-0.154-0.148	-0.043	0.029	0.024-0.033	11.293
11	0.128	-0.021-0.278	1.685	0.022	0.015-0.029	6.112
12	0.142	-0.058-0.342	1.391	0.023	0.019-0.027	11.962
13	0.085	-0.065-0.236	1.11	0.028	0.024-0.033	12.509
14	0.268	0.099-0.436	3.117	0.015	0.009-0.021	4.969
15	-0.002	-0.143-0.141	-0.017	0.022	0.015-0.030	5.745
16	0.094	-0.073-0.261	1.108	0.026	0.023-0.029	15.474

17	0.280	0.126-0.435	3.556	0.006	0.001-0.012	2.339
18	0.116	-0.032-0.265	1.534	0.004	-0.003-0.011	1.138
19	0.213	0.060-0.366	2.735	0.009	0.006-0.012	5.729
20	0.358	0.222-0.494	5.157	-0.001	-0.007-0.005	-0.392
21	0.112	-0.029-0.253	1.555	0.007	0.001-0.014	2.344
	0.141	**-0.018 - 0.302**		**0.019**	**0.013 - 0.025**	

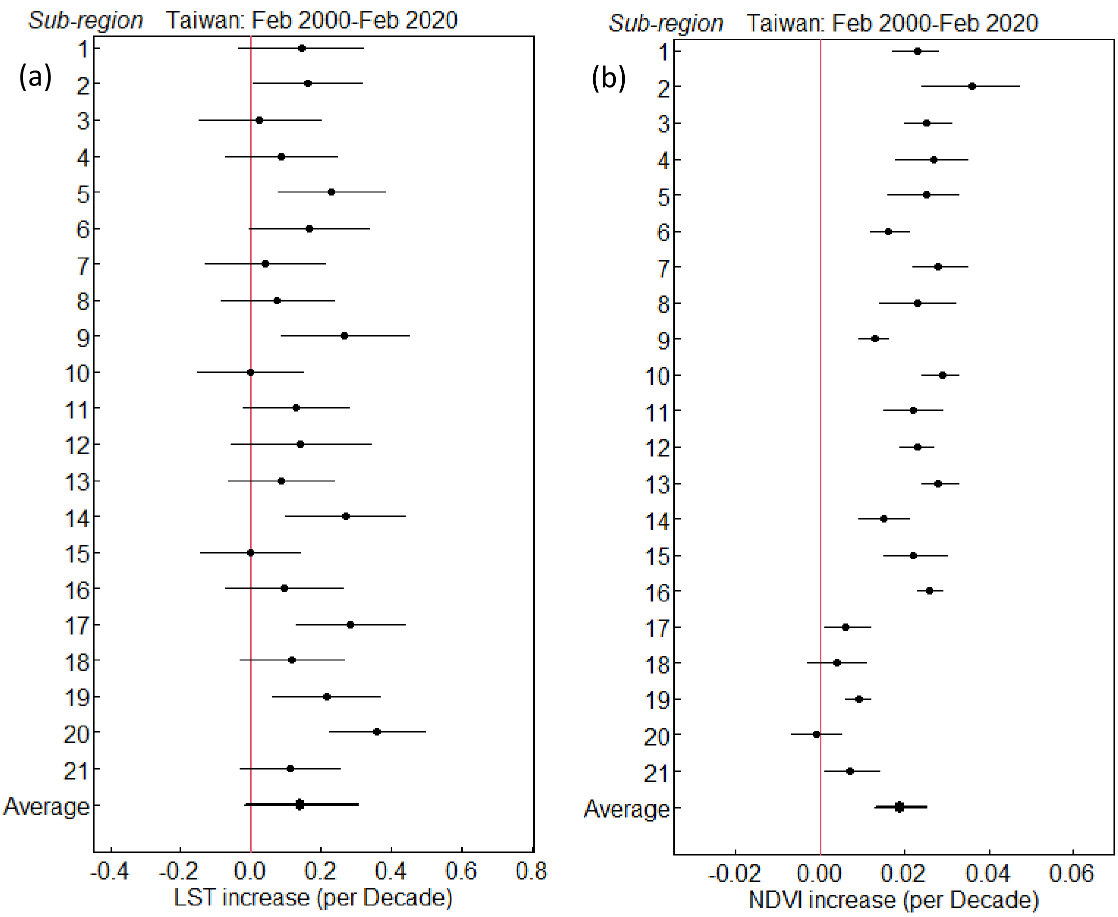

Figure 3.2 Forest plots of decadal LST and NDVI change in sub-region level: (a) the 95% CI range of LST increases per decade of each sub-region and (b) the 95% CI range of NDVI increases per decade of each sub-region.

Figure 3.2 presents forest plots to illustrate the 95% confidence interval range of LST and NDVI increases in the last two decade of each sub-region. The Y axis shows the sub-regions of Taiwan which consist of 21 sub-regions. The X axis shows the increase in LST and NDVI increase per decade. The plot illustrates the average increase of the LST was 0.141 per decade and NDVI was 0.019 per decade.

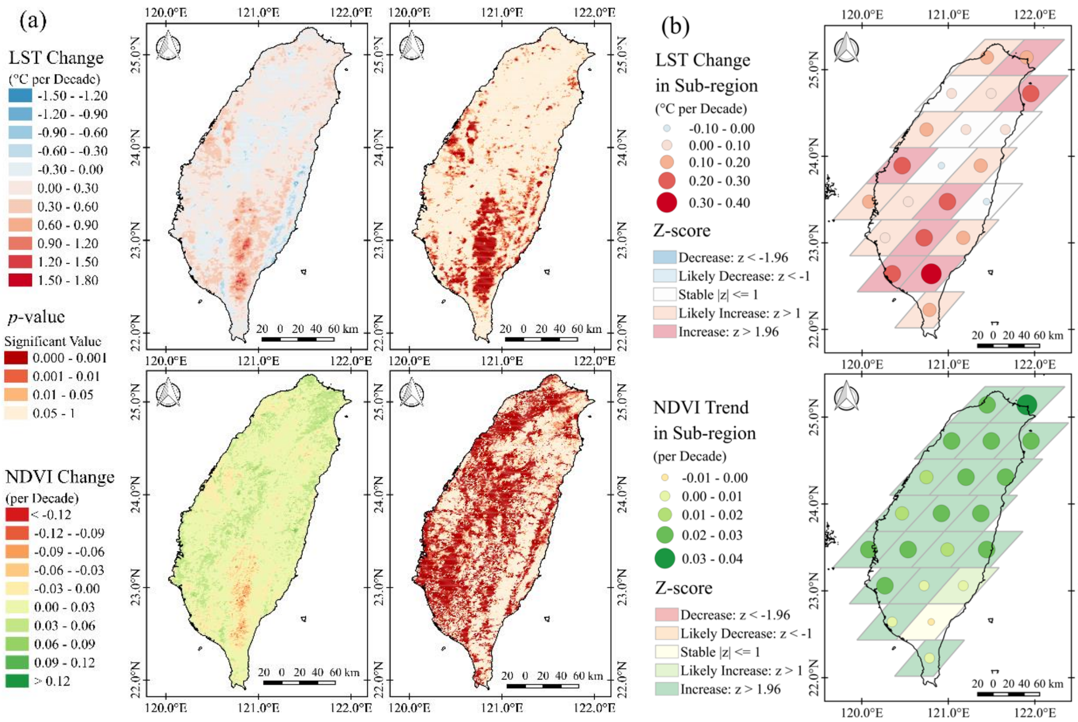

Figure 3.3 Decadal LST and NDVI change in pixel and sub-region level

Figure 3.3a illustrates the decadal of LST and NDVI change map over Taiwan, estimated coefficients, and their correlated *p-value* from a cubic spline model with the zero-knot. The result indicates that a statistically significant increasing LST (> 1.2 °C/dec and *p*-value < 0.05) was shown at the high mountain ranges in the southern part of Taiwan, and slightly increased in the western side of central Taiwan, which is in Taichung city where the industrialized is located. The city center experienced a slight rise in LST, but the neighboring area experienced a significant rise (> 0.3 °C/dec). The noticeable rising LST was also shown in most areas of Kaohsiung city, a big port city, and lowland of Pingtung City in southern Taiwan, including in the flat area of Yilan City which is located in the northeast part of Taiwan Island.

On the other hand, in the narrow Huadong Valley was found a statistically significant decline in LST, similar to the earthen coast of the island. The Danongdafu Flatland Forest Park and some abandoned agricultural areas in Guangfu Township of Hualien City (northern part of Huadong Valley) indicated a considerable decline in temperature (> – 1.2 °C/dec).

In the southern mountainous region and nearby Taichung City, increasing surface temperatures were spatially associated with decreasing NDVI trends (> – 0.03 unit/dec and p-value 0.001). Despite the fact that the total pixels show a slight increase in NDVI, 57.6% of them were statistically significant (0.06 unit/dec and p-value 0.001). Moreover, there were regions where their LC significantly grew up vegetation index (> 0.06 unit/dec and p-value < 0.001) for example, the Danongdafu Flatland Forest Park in Hualien City and the Jiujiufeng Nature Reserve in Nantou City, on the border of Taichung City. The later landscapes are abnormally steep grassy mountains that are simply eroded by rainfall to the jagged peaks form. During the major landslides, this region greatly lost its original vegetation cover caused by the 7.3 magnitude Jiji earthquake in 1999. In addition, its exclusive landscape has been prevented from becoming a nature reserve by the Forestry Bureau since 2000.

Figure 3.3b illustrates 21 the sub-regions of LST and NDVI change map, estimated coefficients, and their correlated p-value (in terms of a standardized normal score, z-value) from the multivariate regression model. Daytime LST and NDVI increase per decade with 95% CI and z-values of each sub-region were summarized in table 3.1 and Figure 3.2. The results from the increased surface temperature conditions (0.1 – 0.4 °C/dec) on seven sub-regions which show in the pastel pink indicated constant results for the pixel-based analysis. Further sub-regions depicting likely increase (rose pink) or stability (white) showed no statistically significant change. On the southern shore of the Taiwan island, increasing greenness trends were displayed across the island, exclude for two regions (in light green and white).

For the whole Taiwan island, the ΔLST varied between – 0.003 and 0.358 °C/dec with the mean of 0.142 °C/dec. Furthermore, the ranged of 95% CI from – 0.018 to 0.302 °C/dec. This statistical figure of the CI overlapping zero which indicates that the LST of Taiwan island was not increase or decrease over time. The ΔNDVI varied between – 0.001 and 0.036 unit/dec and the mean of 0.019 unit/dec. The ranged of 95% CI for the vegetation index increased from 0.013 to 0.025 unit/dec. The CI is above zero, indicating that there has been a significant increase in greenness cover over Taiwan Island over the last 20 years. Our studies offer insight into what has occurred over past 20 years on the Taiwan island at a pixel, sub-region, and region level.

Obviously, LST increased with the decrease of NDVI over Taiwan (Figure 3.4). There was negatively moderate correlation at 0.59 (p-value < 0.001). The greener LC clearly had a moderate correlation, whereas urban lands had a weak correlation (– 0.42 at p-value 0.001). Nevertheless, water bodies were not found to have a correlation.

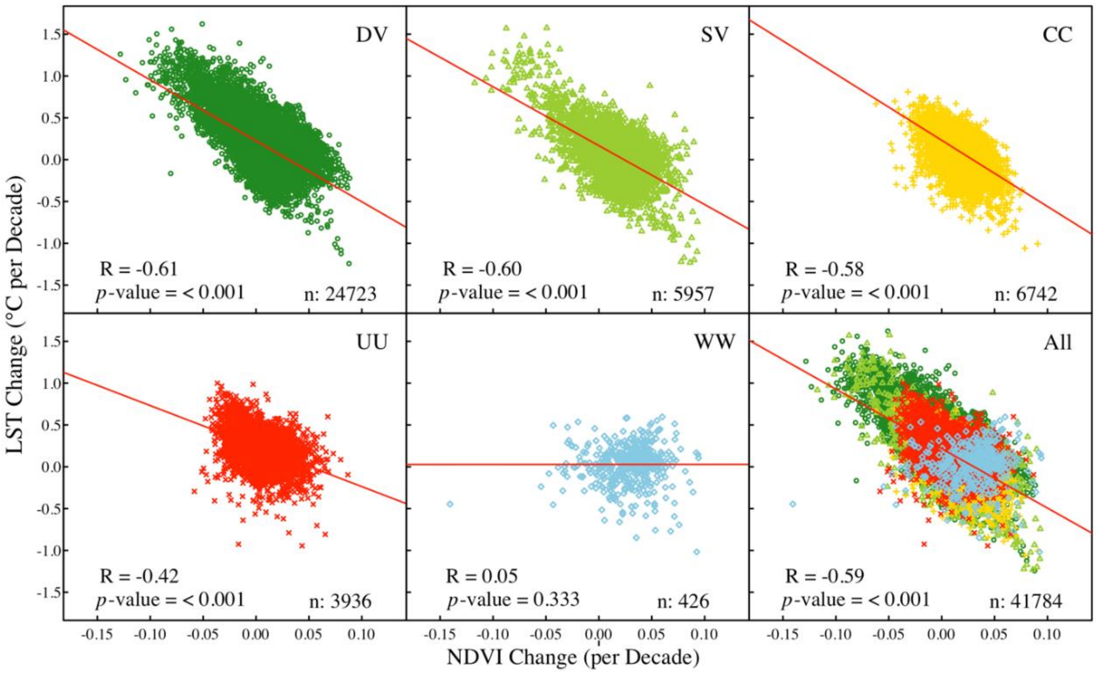

Figure 3.4 Pearson correlation of decadal LST and NDVI change in five major LC classes

3.3 Decadal change of cultivated lands and urban LST and NDVI

Figure 3.5 illustrates the past two decades of cultivated lands and urban LST and NDVI trends in the western plains of Taiwan. The ground surface temperature of urban lands within sub-region 6 show significantly increased. Simultaneously, vegetation index had reduced as expected with the same variation pattern of thermal behavior and plant coverage in other metropolitan settings across the globe. A parallel pattern was discovered in minor urban townships near agricultural areas in the sub-region 9 and Kaohsiung megacity in the sub-region 19, but not in Tainan, the former capital city. Moreover, there was a significant increase for both LST and NDVI in sub-region 16. Several farming actions in the western plain cause an increase of the greenness. Vegetation index in the cultivated areas in all sub-regions has grown up, while surface temperature was not statistically significant increased excluding sub-region 9 and 19. In sub-region 16, the vegetation index coverage on cultivated areas was significantly increased in the last two decades, as a result in stable LST, but not in sub-region 9 and 19 while there was a statistically significant rise in ground surface temperature.

The shape and size of the urban areas and their surrounding lands within the sub-region could vary surface temperature and vegetation trends at the sub-region scale. Furthermore, diverse LU and fertilization in agricultural management, including irrigation in the area of the last two decades, could influence surface temperature and vegetation index cover dynamics in diverse areas. However, it is critical to look into the true drivers of long-term increases in surface temperature and vegetation, specifically LU, local climate, landscape, and ecosystem. Assume the changeability of the landscape and LULC is high. In that situation, investigating of an overall surface temperature and vegetation index trends using a multivariate regression model in a smaller sub-region could offer more reliable and accurate insights, but the costs of computing may be high. Nevertheless, modeling data in bigger sub-regions with less diverse LC and less heterogeneous landscapes may be desired.

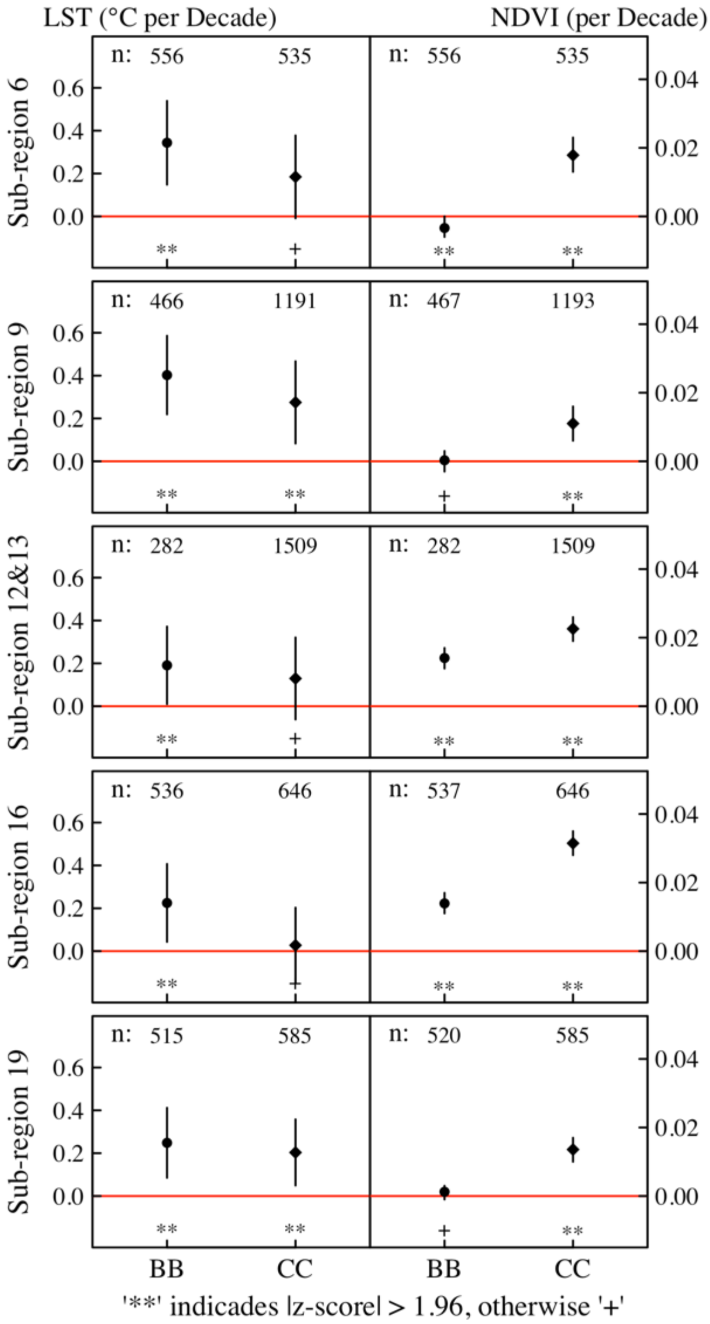

Figure 3.5 LST and NDVI change in built-up and barren (BB) and cultivated cropland (CC) areas inside sub-regions on western plain of Taiwan.

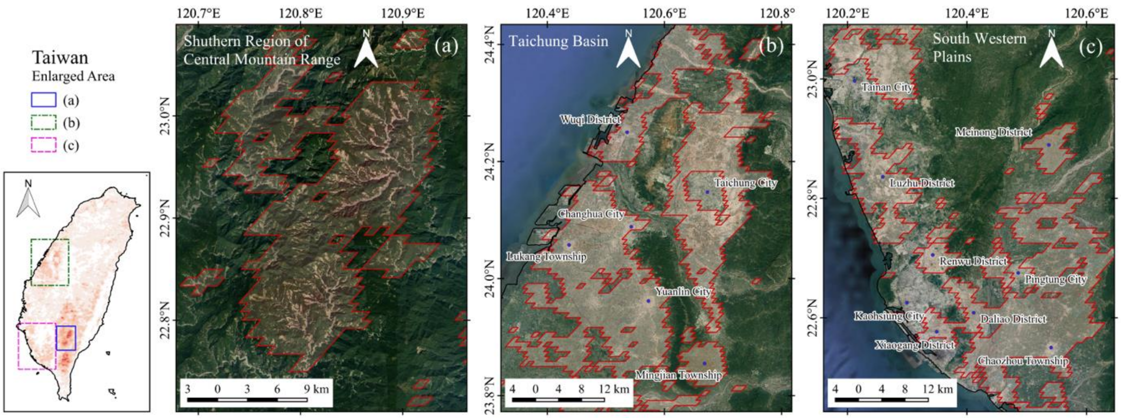

Figure 3.6 Increasing LST in (a) southern region of CMR (LST trend > 0.60 °C/dec), (b) Taichung Basin (LST trend > 0.00 °C/dec), and (c) southwestern plains (LST trend > 0.00 °C/dec).

Note: the Landsat images were retrieved from Google Earth Platform.

3.4 Dynamic Patterns of 20-year Daytime LST and NDVI

In the beginning sector, the natural cubic spline model with zero-knot was applied to filtered $NDVI_{s.adj}$ and $LST_{s.adj}$ time series for all pixel and described the decadal of general trends over Taiwan LC. In this part, the natural cubic spline model with four knots was applied to evaluate the rate of acceleration of these two indices for all pixel. Next, we used a scatter plot to represent the association between these estimated rates of acceleration and the estimated overall trends. Lastly, the equivalent dynamic patterns all over the Taiwan island were demonstrated.

There are five classification patterns of long-term variations based on the scatter plot area (Figure 3.7a). The scatter plot was classified into four quadrants at which a trend and an acceleration rate are zero. First quadrant is the accelerating increase (AccInc) pattern shows both a long-term trends and its acceleration are increasing (both positive estimates), indicating a rapidly increasing dynamic. Second quadrant is the decelerating decrease (DecDcr) pattern is indicated as deceleration decrease trends (both negative estimates). Third quadrant is the accelerating decrease (AccDcr) pattern is indicated in the second quadrant wherever the trend is decreasing (negative estimates), but the acceleration is increasing (positive estimates). Fourth quadrant indicates the decelerating increase (DecInc) pattern. It is showing a rising tendency with deceleration rate. These four quadrants excluded an area of the Stable pattern, specified as a variation rate of ±0.3 °C/dec for LST and ±0.03 unit/dec for NDVI and the acceleration rate of ±0.5 unit/dec^2 for both. The results show 41.1%, 39.8%, 17%, 1.6% and 0.5% of Stable, AccInc, AccDec, DecInc and DecDec patterns of LST, respectively. On the other hand, the majority of NDVI patterns indicated to be stable (76.5%). The AccInc and DecInc patterns of NDVI represent about 9% and 9.4%, respectively. The DecDcr pattern of NDVI was found only 1.1%.

When comparing the linear trend distribution of the LST and acceleration pattern, most of the AccInc pattern pixels (Figure 3.7b) corresponded with the rising linear trend pixels (as illustrated in Figure 3.3a). The rapid increase of LST did not only show in the urban lowland and nearby agricultural lands, but similarly display in the forest that covers mountain ranges and dense vegetation. Correspondingly, many pixels with the AccDcr pattern were also spatially matched with declining trend pixels. The results from this study revealed that in some areas the conditions of surface temperature in the first decade were rapidly declining, seemed to increase gradually in the last 10-year period, and tended to be increased in the future. In addition, the DecDec of LST pattern was indicated at Linhousilin Flatland Forest Park and nearby abandoned agricultural plantations in Pingtung City which is located in the Southern Taiwan. There was another area that indicated the same pattern found at Aogu Wetlands Forest Park which located at the mouth of the Beigang River, the border between Chiayi and Yunlin City in the middle of western Taiwan. The wetlands were represented to be sugarcane plantations and farmlands. Nevertheless, almost all of the land was not appropriate for agriculture because of the seawater invading ground water and finally turning into a wetland throughout high tide and open woodland.

Moreover, 76.5% of Taiwan land reveals a stable pattern of vegetation with no rapid or slow variations over the past 20 years (Figure 3.7b). In some areas of the study, there were other NDVI patterns found. Several clustered regions of rising vegetation with a high acceleration rate, denoted as the AccInc pattern, were over the mountainous land in the eastern part of New Taipei City, during western flat plains with fertile cultivate areas, and along various massive river floodplains, such as Dajia River, Dadu River (also known as the Wu or Black River), Da'an River in Miaoli City, Houlong River and Touqian River in Hsinchu City, flowing through Taichung City. Furthermore, it would be pointed out that the Gaoping River, the biggest river in southern Taiwan by drainage land with its tributary rivers; Laonong, Zhuokou, and Qishan Rivers, indicates two different acceleration patterns; AccInc and AccDcr. The southern mountain ranges encountered a dramatic decrease of vegetation cover in the first decade and a gradual gain up in the latter decade.

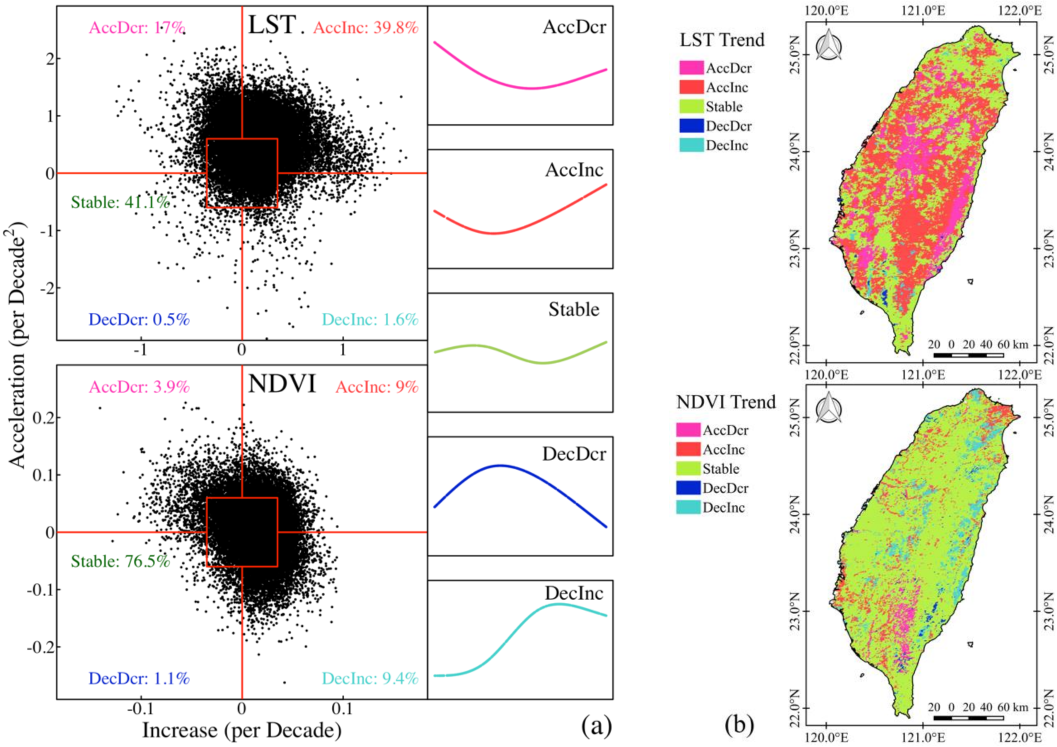

Figure 3.7 (a) Five classifications of ΔLST and ΔNDVI patterns over 20-years period and (b) their distributions on Taiwan Island.

3.5 LC Change and Elevation

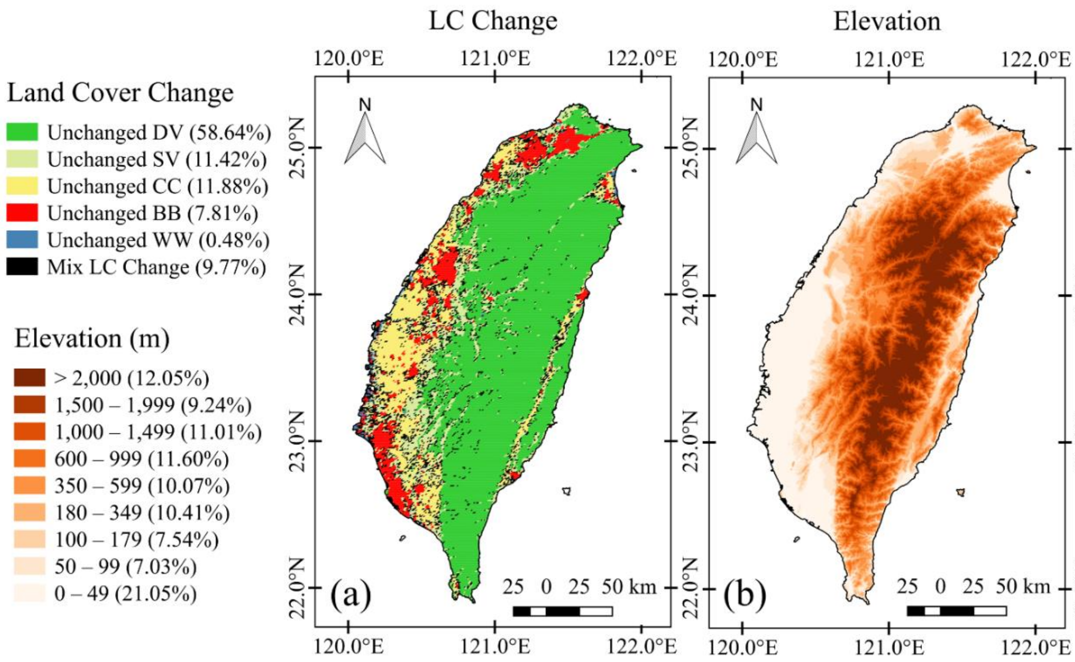

Figure 3.8 (a) LC change of Taiwan (from 2001 to 2019) accosting to five re-classified groups of 13 IGBP LC types, and (b) nine levels of elevation.

Figure 3.8 illustrates the distribution of LC change in Taiwan between 2001 and 2019 and the elevation, which was classified into nine classes. Considering the conversion of LC, the Unchanged DV area covered 58.64% of the island and found most in the mountain range around 1090.50 m above sea level by median (IQR: 527.75 – 1839.25 m) of all unchanged DV areas. Unchanged CC, BB, and WW lands contributed by 11.88%, 7.81%, and 0.48%, respectively, of the island area. Most of them were located in the land whose elevation was lower than 50 m and covered approximately 21.05% of the island area. The overall elevations by the median for unchanged CC, BB, and WW lands were around 27 m, 22 m, and 2.5 m, respectively. Most of the unchanged SV land was found in the higher elevation (around 120.5 m by median) and contributed by 11.42%. Nearly two decades, LC of Taiwan has changed only 9.81% of the entitled island, and the majority of the transformed areas were found in the land that its elevation was around 90.5 m by median (IQR: 24.5 – 259.0 m). Areas with its LC had transformed from SV to CC were the most land conversion as 34.51% of the LC changed areas. LC change between SV and DV was the second conversion form which was around 19.93%. Shrinkage of DV area that transformed to SV land and the increases of SV land converted from the cultivated LC (CC) were contributed as the same amount as approximately 12.94% as described in Table 3.2.

Table 3.2 Transition matrix of LC change between year 2001 and 2019.

	LC Group	2019					Total Pixel
		DV	**SV**	**CC**	**BB**	**WW**	
2001	**DV**	24499	533+	15	2	14	25063
	SV	821**	4771	1421*	272	50	7335
	CC	41	534++	4965	129	8	5677
	BB	0	49	51	3264	88	3452
	WW	10	37	2	4	199	252
	Total pixel	25371	5924	6454	3671	359	41779

Significant Change (*) SV to CC, (**) SV to DV, (+) DV to SV, and (++) CC to SV

3.6 Decadal of daytime and nighttime LST Change

The change of LST in a decade, which was estimated using linear regression model fitting for each filtered seasonally adjusted LST time series (each pixel), and its corresponding null hypothesis significance testing (p-value) are illustrated in Figure 3.9. The daytime LST trends range from -1.24 to 1.62 °C/decade, and their average was 0.14 °C/decade. The daytime surface temperatures that increase more than 1.00 °C/decade with statistical significance (p-value < 0.05) were found in the southern part of the mountain range, as shown in Figure 3.9(a). Some moderate increasing daytime temperatures (0.30 – 1.00 °C/decade) with statistically significant also found in the southern mountain range and most in the cropland (39.64%) and urban area (42.64%) which located around the middle and southern part of western lowland (< 50 m above sea level). There were 29.35% of decreasing LST trend throughout Taiwan island. However, there was only 4.21% of all areas where its surface temperature was decreasing with statistically significant results, which found most in the valley and lowland along the earthen coastline of the island. The average nighttime LST trend was 0.31 °C/decade and ranged from -1.05 to 1.00 °C/decade. More than 72.14% of all areas that its surface temperature was a statistically significant increase. The increasing surface temperatures were found throughout the island except for the south-earthen region, where the surface temperature trends were declining (7.27% of the entire study area). However, only 21.06% of LST trends in this region were statistically significantly decreased.

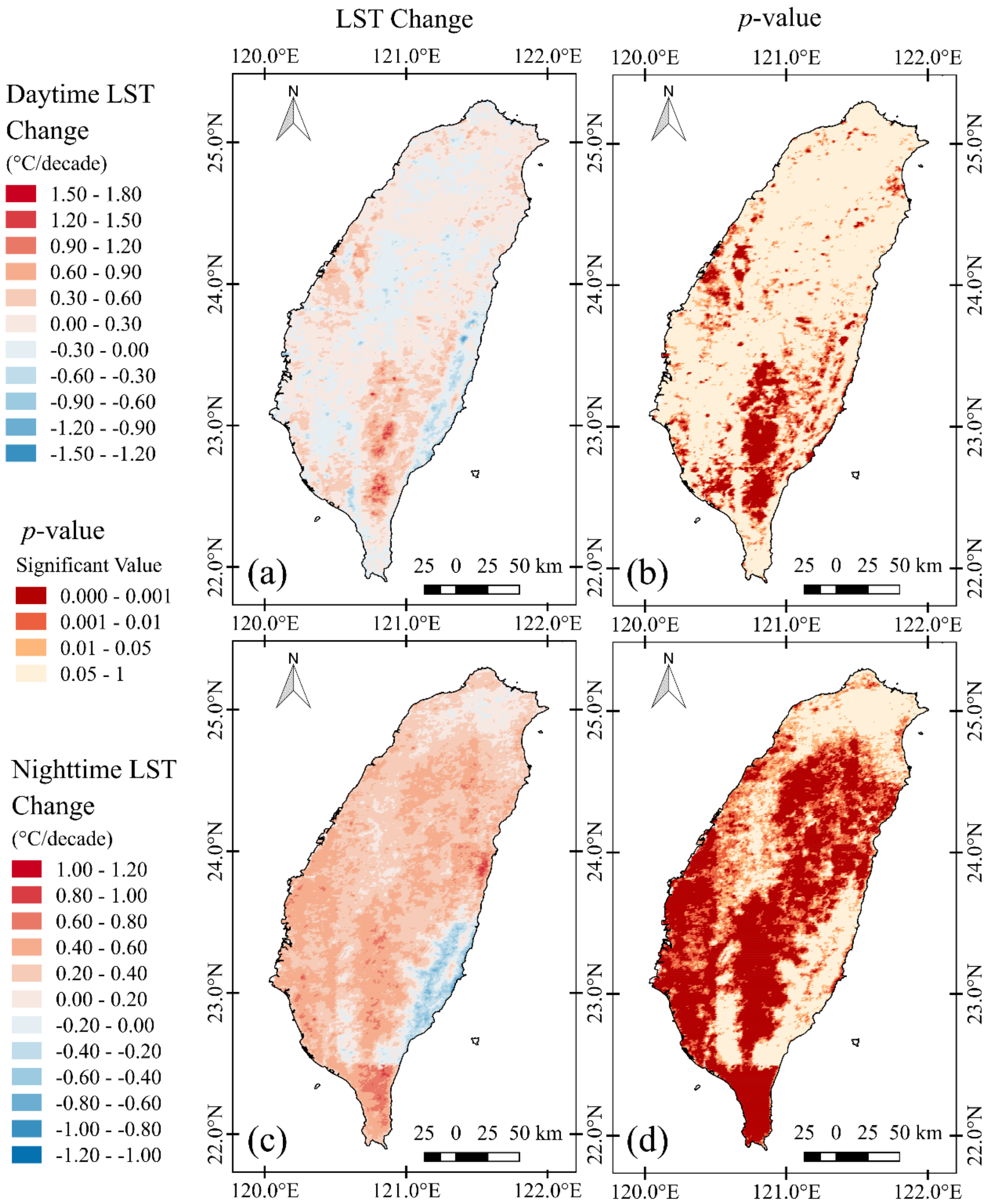

Figure 3.9 Distribution of decadal (a) daytime and (c) nighttime LST change in Taiwan, and distribution of corresponding statistical significant value (p-value) of (b) daytime and (d) nighttime LST change.

3.7 Linear Regression Analysis with Weight Sum Contrast of Decadal LST Trend

Figure 3.10 illustrates the estimated mean of daytime and nighttime LSTs with comparative confidence intervals after adjusting for elevation and LC change with the overall mean for each factor. Graphs in the first column of Figure 3.10 show the effect of elevation, whereas graphs in the second column show the effect of LC transformation on decadal daytime and nighttime LST trends, graphs in the first and second row, respectively. The horizontal red lines indicate the overall mean by simple average LST trends from all pixels. The green dots indicate crude means which were the mean of LST trends in each group of elevation and LC change. The label “r-sq:” shows adjusted r-squared from regression fitting with separated determinants. The label “Overall r-sq:” denotes adjusted r-squared from the regression model adjusting for elevation and LC change factors. The label “n:” indicates the percentage of unequal sample size for each level of factors.

The overall mean of daytime and nighttime LST trends was 0.14 and 0.31 °C/decade, which implies that the surface temperatures in the study area were escalating. Graphs in the first column clearly show an effect of high elevation (>600 m) in both daytime and nighttime LSTs. In the daytime, there was a sizable difference by comparing mean in each difference of LC conversion and the *p*-value, which for the difference between two or more population means, confirms that the hypothesis that the population means are equal can be rejected. The mean of LST trends in the unchanged BB area and mean of LST trends in areas where their LC conversed from DV to SV land was above average as 0.24 °C/decade, which is two times higher than the overall mean. In contrast, mean of LST trends in conversion land from SV to DV land was lower than zero as -0.04 °C/decade and different from the overall mean by 0.16 °C/decade. Mean of LST trends in the other groups of LC change showed an insignificant difference from the overall mean. However, their confidence intervals were not overlapping each other or riding on the overall mean. The difference in LC change does not affect nighttime LST trends. The mean of LST trends in all different groups of LC change was very close to the overall mean. Some of their confident intervals overlapped each other and crossed the overall mean line, suggesting that there was insufficient evidence of the difference.

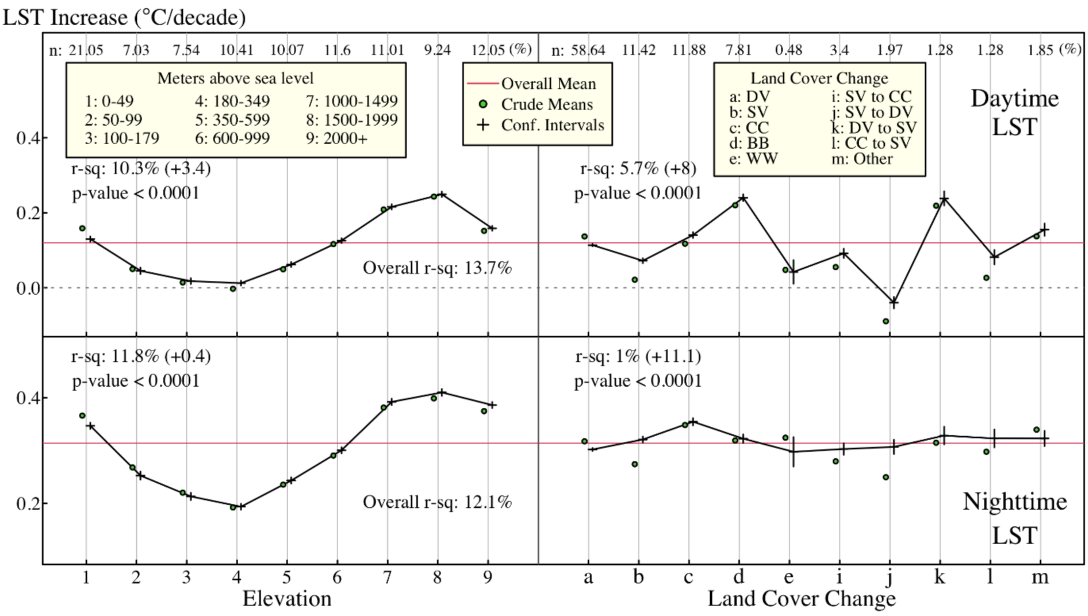

Figure 3.10 Mean and confidence intervals of daytime and nighttime LSTs based on a linear regression model fitting using weighted sum contrasts with elevation and LC change groups as determinants.

3.8 The effect of elevation and LC change in the north and south region

Overall, the surface temperatures in the study area were escalating, especially at nighttime that up to 0.31 °C/decade on average. Analysis of LST during 20-year study period demonstrated that the change of nighttime LST mostly increased all over Taiwan Island when comparing to daytime LST. Over 73.67% of the study area that it’s nighttime LST increased with statistically significantly whereas daytime LST increased only in 26.72% of the study area. Considering Figure 3.8a and Figure 3.9c, the distribution of increasing LST trends display a roughly spatial relation with LC change. However, LC type and the form of LC change had a small effect on the variability of nighttime LST trends which had an insignificant differences, as shown in Figure 3.10. Only mean LST in the BB area (urban, built-up, and barren) showed considerable difference from the overall mean. On the other hand, daytime LST trends were substantially varied in various LC types and their change patterns.

Transformation of vegetation cover in both ways, deforestation and afforestation, strongly impact on the daytime LST trend. There was around 58.65% of the study area that was covered with dense forest and more than 71.40% of that forestry area was located above 600 m from sea level. However, both daytime and nighttime LST in 20 years had increased overall.

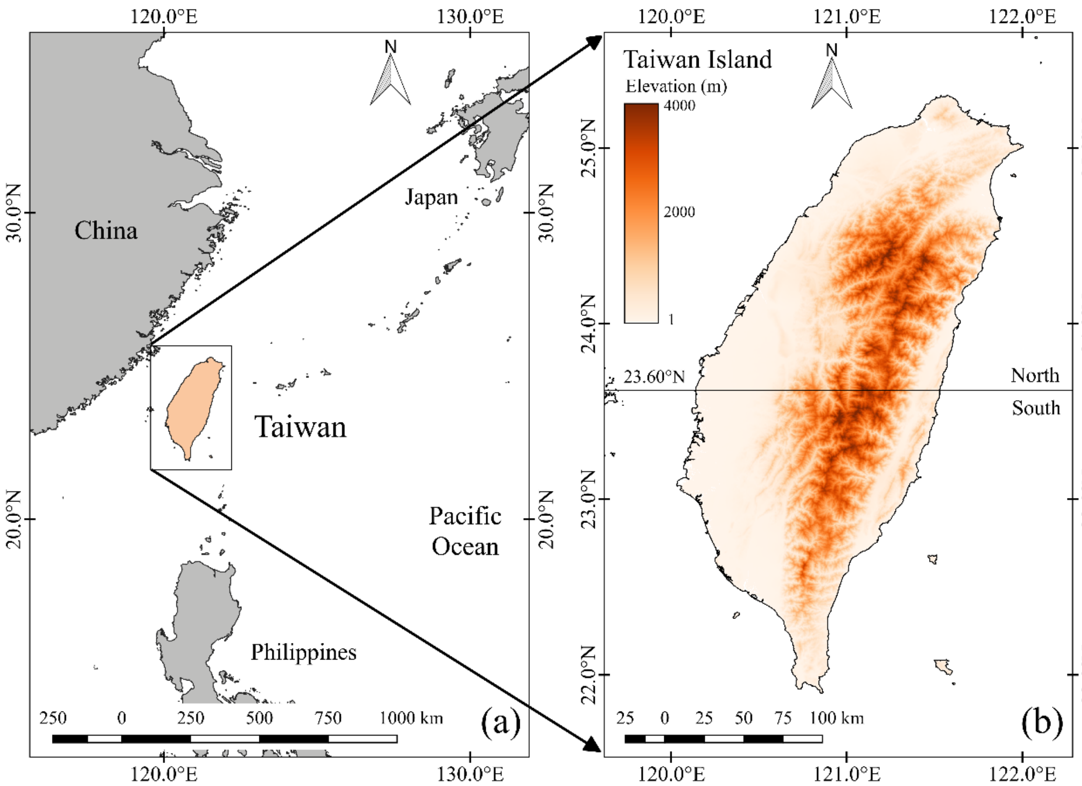

Figure 3.11 The map of Taiwan divided in the north (above) and south (bottom) regions.

According to elevation graphs in Figure 3.10, both daytime and nighttime LST trends in areas over 1,000 m above sea level, primarily unchanged DV LC, appeared to escalate significantly. However, when the study area was divided into north and south regions by 23.60°N latitude, as shown in Figure 3.11, areas over 600 m only in the south regions advocated the overall daytime and nighttime LST trend. Figure 3.12 shows the effect of elevation and LC change in the north and south regions on the daytime LST trend. It reveals that not only the high elevation (>600 m) area in the southern part of the island strongly contributed to the increase in LST trend, but also the class of LC conversion. The pattern of increasing/decreasing temperature at each level of elevation and LC change factors was similar to the daytime LST increase for the entire Taiwan island, as shown in Figure 3.10.

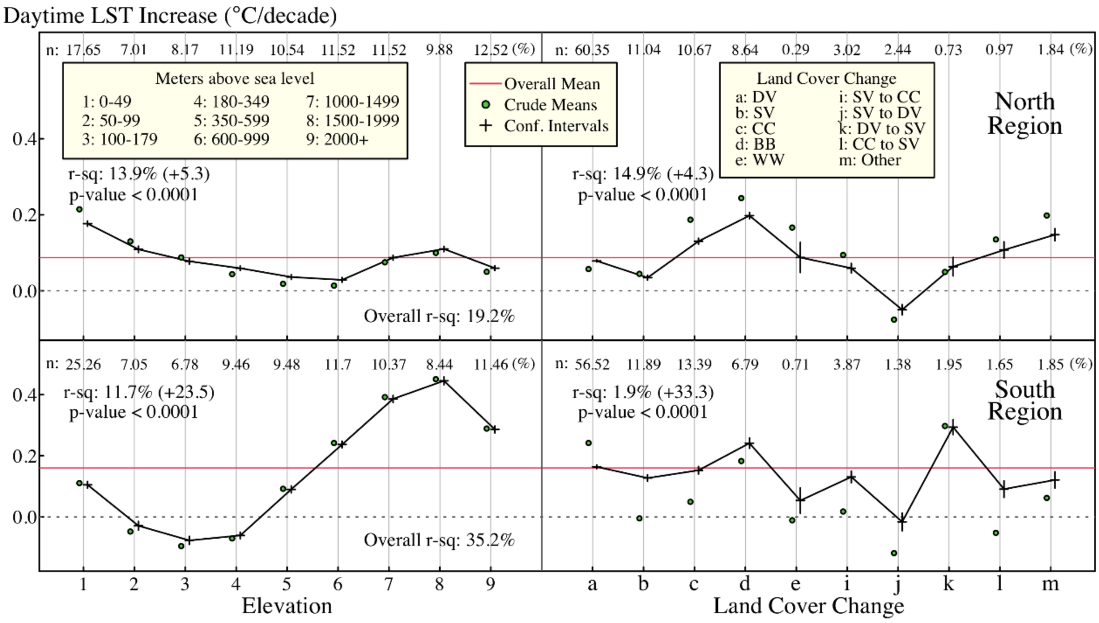

Figure 3.12 Mean and confidence intervals of daytime LSTs in the north (above) and south (bottom) regions.

LST trends in areas over 1,000 m above sea level, which were mostly unchanged DV LC, appeared to increase significantly. Figure 3.13 reveals the LC change due to major soil erosion and massive landslides in many steep valleys around the southern mountainous region.

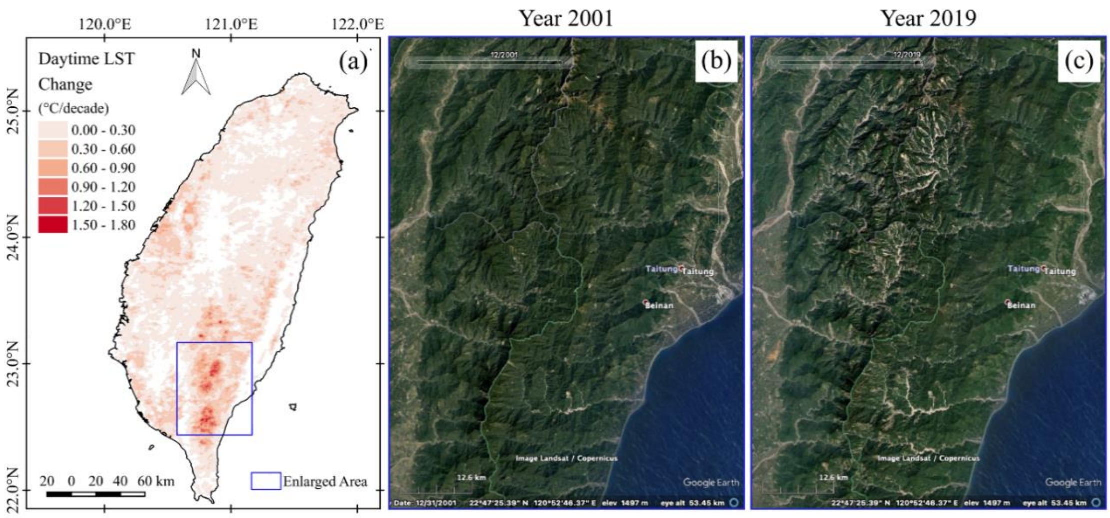

Figure 3.13 (a) enlarged area of interest where high daytime LST increased with statistically significant and high resolution airborne imagery from Goggle Earth platform in (b) 2001 and (c) 2019

Chapter 4

Discussion and Conclusion

This chapter consists of the discussion, conclusion, limitation, suggestions and recommendations for future studies.

4.1 Discussion

By applying a suitable number of knots to the cubic spline model, we successfully modeled LST and NDVI seasonal patterns, changing trends, and dynamic patterns over Taiwan from 2000 – 2020. Therefore, not only the rates of the two indices were revealed, but their acceleration and deceleration rates were also explained. There were previous studies of LST that had been applied with the same approaches for investigating time series and reported a notable rise somewhere (Fitrahanjani *et al*., 2021; Wongsai *et al*., 2020b; Hamoodi *et al*., 2019; Ullah *et al*., 2019; Islam and Ma, 2018), and it is not remarkable to Taiwan. This analysis investigated the changing rate of ground surface temperature at island level, sub-region, and 1-km pixel level. Even though the average rising LST was 0.142 °C/dec and its 95% CI verified that the last 20 years through the study area, the mean surface temperature did not change. In contrast, the cover of vegetation index on Taiwan island was noticeably increasing with statistical significance.

4.1.1 LST and NDVI Trend at Sub-region Scale

The result indicated that a cooling or warming tendency changed to more obvious when analyzing in sub-regions. As a result, there had been experienced warming surface temperature trends of two urban context sub-regions. Sub-region 5 in the northeastern Taiwan covers most of the Yilan Plain, where Luodong Township and Yilan City have high citizen densities. Moreover, sub-region 19 covers part of the Pingtung and Chianan Plain, covering most regions in and nearby Kaohsiung, including its surrounding Pingtung City in the Taiwan southwest. It is known as a tropical megacity for its international port and industries with durable influences from urban heat island (UHI) and drastic surface temperatures (Huang and Chen, 2020). Furthermore, there has been tightly constructed in the city with high buildings and paved roads similar to other cities areas in Taiwan that are influencing by the UHI warming (Shih *et al*., 2020; Hsu *et al*., 2002; Chen *et al*., 2017; Chen *et al*., 2016; Kato *et al*., 2012; Lin *et al*., 2008).

There was a statistically significant increase of LST in sub-region 9 which covers the Changhua City and Yunlin City areas in the Changhua Coastal Plain. These regions are the major significant Taiwan agricultural land. The study result verified that the finding found by Chen *et al*. (2013) that the western central Taiwan has been facing warming trends of LST because of the variation of the ground transform to agriculture and urbanization. The variable of surface temperature has greatly influenced this area, particularly in coastal areas with violent land subsidence that always face with floods during each typhoon duration (Lee *et al*., 2016). Groundwater over-pumping and saltwater incursion lead to the formation of wetlands in many agricultural areas. The steady occurrence of fragmented small marshland patches surrounding the agricultural land in this area could influence the rise in surface temperature rather than the aggregated patches of bigger sizes that indicate low and steadier surface temperature (Muro *et al*., 2018; Cai *et al*., 2016). Massive wetlands consist of larger thermal inertia and capacity, decreasing thermal radiation and the exchange intensity between them and their neighboring. The surface energy budget dynamics over wetlands influence ground surface temperature processes and affect local climatic circulation. It influences the resources of thermal spatial dissemination and significantly distributes, throughout evaporation, to the cooling of farming landscapes adjacent to wetlands (Du *et al.*, 2019; Huryan *et al*., 2014). Nevertheless, the latent capacity and appropriate heat fluxes kept in a column of water surface in a small and shallow wetland are limited. As a result, it is a speedy rise in LST. Extra heat energy obtain from solar radiation was released throughout the day that provides a high of LST in the wetland water body and causes rise in surface air temperature and adjacent LST in the local energy balance (Jia *et al*., 2020).

The Central Mountain Range (CMR) of Taiwan southern region, surrounded by sub-region 14, 17, and 20, reveals remarkable surface temperature variations. A notable variation with 0.358 °C/dec, correlated with the enormous reduction of vegetation and was found in sub-region 20. Typhoon Morakot heavily destroyed the coverage of the origin plant in this area from the hill area in 2009. Moreover, it generated excessive precipitation through the southwest and northeast of CMR, causing intensive catastrophic landfalls and drastic mudflows in the southern region (Chien and Kuo, 2011; Tsou *et al*., 2011; Agyakwah and Lin, 2021; Yang *et al.*, 2018). Consequently, the wide areas of rocky bare soil are revealed on steep hillslopes. The massive scar of the mountainous landscape can be noticeable from aerial or satellite imagery. However, reducing of vegetation cover is one potential cause of ground surface temperature in this mountainous terrain to increase with high acceleration over the past decade of the study period. Therefore, NDVI in this high-altitude area indicates a rising trend in the last decade and has an increasing direction in the future. It indicates that the landscape and vegetation in this region have steadily recovered.

Interestingly, several Taiwan sub-regions had faced warming ground surface temperature. However, several mountainous areas in the northern part of sub-regions 1, 2, and 4 cover greener LC with significant warming temperatures. This finding is in parallel with the result implemented by Tsai and Yang (2016), which reported that the northern part of Taiwan unveiled a rising of vegetation pattern contributed by the observed increase in rainfall during 1982–2012. When precipitation was overwhelming, the roots of the plant produced oxygen-free breathing that immediately influenced the absorption proficiency of nutrients and water of plant and also reduced light which negatively influenced the photosynthesis of vegetation and stunted the growth of the plant (Ye *et al*., 2016; He *et al*., 2020). Therefore, the increase in rainfall in this mountain ranges area, which is comparatively short in water properties and has directed to higher soil water content and moisture conditions of vegetation canopies. Consequently, the rising of rainfall was useful to the vegetation growth. Moreover, the suitable combination of air temperature and precipitation influence vegetation growth. The sufficient warmth, overwhelming precipitation, and accelerated physiological activities of vegetation put the plants on nicely and increase the vegetation index (Kong *et al*., 2017; He *et al*., 2020). Hydrothermal conditions in the northern region of Taiwan with simultaneous rise in air temperature and rainfall might increase of efficiency light consumption and humidity obtainability for vegetation and consequently lead to growth in the plant (Piao *et al*., 2003).

The seasonal mean of LST and NDVI were a significant positive association for all seasons. According to Piao *et al*. (2003) found that their result indicated the long–

term rise of NDVI over China during 1982–1999 and was consistent with increased LST and rainfall in summer. The growth in vegetation and precipitation that positively associates with air temperature and might crucial or as a minimum partially account for statistically significant increase in LST in this area. In the meantime, near-surface air temperature and LST have a direct correlation, and the relation between ground surface temperature and vegetation water content is intensely positive on green plants area (Guha *et al*., 2020).

4.1.2 LST and NDVI Trend at 1-km Pixel Scale

Our findings at the pixel level showed spatial phenomena for instance urban growth in various places of the Taiwan western plains. The notable growth of the significant warming areas was correlated with an edge-expansion (or sprawling) form of urban expansion, wherever a recently developed urban area spreads out from the full expansion urban patch (Xu *et al*., 2007; Liu *et al*., 2016). Surface temperature in Taichung city center, where it's interior is the high density of road networks and buildings which has slightly grown up in the last two decades but was not statistically significant. On the other hand, there was a statistically significant warming of surface temperature trends were found in suburban areas nearby the city center. This comprises major coastal suburbs in western Taichung City (Qingshuim, Wuqi and Longjing districts) which is the second-biggest Taiwan port is located. The similar event was also happened in the other two urban areas which are Tainan and Kaohsiung City located in the southwestern Taiwan. The intrusion of metropolitan area on neighboring sub-metropolitan area is the significant source of the UHI influence in several large cities around the globe (Qiao *et al*., 2014; Zhao *et al*., 2016; Imran *et al*., 2019; Chen *et al*., 2020).

The results from our finding also displayed the large patches of several levels warming regions over the cities and agricultural areas in flat plains of Changhua City and Pingtung City while their vegetation was gradually reducing. These regions are categorized by small urban townships surrounding each other with suburban residential areas and farmlands in between. LC diversity within a square kilometer area indicates the degree of variation of surface temperature change. Moreover, the diverse degrees of an increasing portion of the impervious surface area caused a diverse quantity of increasing in LST trends over the period (Wongsai *et al*., 2020a).

Investigating LST or NDVI trends of long-term at pixel level could offer intuitions into and elevates responsiveness of LULC variations and land activities in particular regions. For instance, there were two rural township areas which are in Mingjian Township in western Nantou City and Meinong District in Kaohsiung City, facing high accelerated increasing ground surface but the coverage of NDVI loss insignificant. Mingjian Township of Taiwan is the biggest tea-production area. Minor-scale irrigated tea farms contribute 26.1% of the township area, and 37.1% are other popular plantations, for example betel pepper, Chinese yam, ginger, and pineapple (Wang *et al*., 2021). The major agricultural production is rice in the southern area of Taiwan (Chiang and Liu, 2013). Furthermore, Meinong Township had a rice production area of 7,000 Hectares (ha) during 1960 and 1970. Nevertheless, in the late 1990s the production of rice in Meinong District down to haft of its area due to overproduction. A lot of paddy fields were twisted into pounds to farm white water snowflakes, tropical fruit plantations, and vegetable shade net houses. Suchlike LULC variation and agricultural LU activities for example irrigation systems and agricultural management practices that might affect the increasing of LST in these areas require to be further studied. Initial extensive policy responses, comprising sustain actions and systematic, are desired to protect the disastrous results of local climate situations on cultivated production, which is a major source of the local economy.

4.1.3 LST and NDVI Acceleration Trends at 1-km Pixel Scale

The rise of LST trends as the NDVI rates decrease for each LULC type, but their correlation coefficients associated with LULC types are distinct (Yue *et al*., 2007). There was a strongly negative association found especially in the urban land (Guha and Govil, 2020; Guha *et al*., 2018; Kumar and Shekhar, 2015). The results of our study pointed out that the long-term surface temperature and vegetation trends had negative associations in different LC types at a pixel scale, excluding in water bodies and wetland areas. The associations were stronger in dense forest compare to built-up area. It recommends that the reduction of vegetation index in the forest area causes more significant LST warming than that in another areas.

The LST trends acceleration was first demonstrated using a quadratic regression model, resulting in two patterns which are accelerating and non-accelerating patterns (Sharma *et al*., 2018a). According to Ismail *et al*. (2019) and Wongsai *et al*. (2020b) recently applied cubic spline function to investigate the acceleration of LST trend. Wongsai *et al*. (2020b) were the first to model the acceleration rate from the coefficients of the cubic spline function, as presented in Equation 4. This method was applied by Devi *et al*. (2021) to investigate the LST acceleration variations in Britain Island, Papua New Guinea. These similar approach was adopted to examine the dynamics of LST and

NDVI trends in the past 20-year of this study. Furthermore, we classified into five LST and NDVI variation patterns by the direction of change and its acceleration rate in this analysis. Such patterns obviously illustrated the different dynamics of long-term LST and NDVI trends and showed the possible trend in the predictable future. These approaches provided statistical implications that indicate interesting intuitions in LST and NDVI trends and their acceleration patterns on the Taiwan island in the past 20 years.

4.1.4 Confounding and Adjusted Comparative Mean

The effect of elevation on daytime and nighttime LST was similar. Means of daytime and nighttime LST trends at lowland (< 50 m) and land that higher than 1000 m were above the overall mean. The sizable rise of average LST trends in lowland was contributed by the built-up and cultivation LC. Although, the urban and cropland area mostly has not expanded or changed as informed in Table 3.1. However, the increasing of built-up and impervious surface density in 1 x 1 km2 during 20 years of study period may cause the rising trend of LST, especially in the daytime. The surface temperature of land in high elevation is generally lower than in the lowland due to the local climate, types of LC and utility of land (Phan *et al.*, 2018). If there was no change of LC, LSTs trend to decline corresponding to higher elevation. From our result, 33.7%, 24.51% and 15.80% of unchanged DV, SV, and CC land, respectively, (74.01% in total) were found within the areas that their elevations were between 50 and 350 m above the sea level (elevation level 2 - 4). Moreover, the mean of LST trends in deforestation or degraded forest area (land converted from DV to SV), which was mostly found in elevation level 5 and 6 (IQR: 217 – 972 m with median at 480 m) escalated the LST trend. This implies that geographical relation between elevation and LC type at the local site affects the dynamic of LST. If the correlation between these two factors was disregarded and their effects were analyzed separately, those results may not be accurate and comparable. In this study, elevation was associated with LC change in the data and distorted the association between LC change and LST trends which issued confounding. A confounding variable influenced both a determinant and an outcome variable, and thus can affect that association between them. The testing result from 10% rule of thumb informed that the parameter estimated for LC change factor in all levels had percentage change more than 21% from the unadjusted, or crude, estimate (from simple linear regression) to the adjusted estimate (from multiple linear regression). This confirmed that the association between LST trends and LC change is confounded by elevation.

As mentioned in section 2.4.5 that a two-sample t-test (for the comparison between two groups of sample size) and ANOVA (for determining whether three or more populations are statistically different from each other) are not appropriate for comparison means of factors that might affect each other. The regression model could be applied to investigate the correlation between multiple covariates and a numeric dependent variable. This method could be used as a multiple linear regression to realize through confounding and separate the association of interest (Pourhoseingholi *et al*. 2012). Moreover, there were unequal and unbalanced sample size of LC change in the study area. Since sample size in many levels of LC change (WW, SV to CC, SV to DV, DV to SV, CC to SV and other) was small and some levels were under-represented, which biased the mean in level of the factor of interest, as presented by the difference between crude mean and adjusted comparative mean with “democratic” confidence intervals. The weighted sum contrasts method corrects this bias and gives the adjusted means of LST trends for each level of the factor of interest which can be obtained simply by fitting the model using weighted sum contrasts and omitting the terms from all other factors. Graphs in Figure 3.7 accurately show how LST trends vary with LC change after accounting for elevation (as the confounding factor) which more accurately reflects the population and clearly revealed the effect of elevation and LC change on daytime and nighttime LST trends.

However, using nighttime LST data may be suitable for long-term regional and global climate change study because LC and their change over time had a minor effect on LST increasing. This result supports the previous study in a smaller study area of Wongsai *et al.* (2020) where the ANOVA test in their study suggested that there was weak evidence that changing temperature amount groups of LC and their change pattern were different. Although, ANOVA analysis in their study was not adjusted for unequal sample sizes.

4.1.5 Influence of LC Change and Elevation on LST Trends

The physical change of LC in the southern mountainous region was noticeable since 2005 and this natural phenomenon was clearly visible from historical imagery in Google Earth platform after 2009. Typhoon Morakot had damaged Taiwan in 2009, especially in southern Taiwan. The moving storm produced amounts of rainfall, mudslides, and flooding. Furthermore, it killed many people and damage agricultural area (Chien and Kuo, 2011; Wu, 2013). The transformation of the hillside and the base of the valley covered by dense vegetation become into the rocky and bare soil surface caused an increase in its surface temperature in this part of Taiwan. Although, LC around this region was unchanged during 2001 to 2019 based on MODIS LC data. It might be that the total area of LC change did not dominate the unchanged area within 1 x 1 km2 area, but the substantial quantity of change area, especially conversion from vegetation cover to built-up and bare land, and its spatial heterogeneity could significantly increase its surface temperature (Wongsai *et al.*, 2020).

However, after a decade of sugar cane cultivation, a number of flora had been changed into flatland forests and open-woodlands below active envelopment in vegetation area afforestation by the Forestry Bureau from the time when the beginning of the 21st century. A comparable LU transformation was also found in Linhousilin Flatland Forest Park and nearby post-agricultural lands in Chaojhou Township of Pingtung City (the tourism and agriculture city in Southern Taiwan). Such variations need for future studies to be observed the influence of plantation change, urban expansion, and physical environment variations (e.g., LU variations, runoff changes, storm, fire, landslide, extreme rainfall, and deforestation), but those variations are not within the current study scope.

4.2 Conclusion

LST in Taiwan has faced warming in many regions, especially in the Central Mountain Range of the southern region, north-eastern, central-western, and south-western (Chianan and Pingtung Plains) but decreasing in the Huadong Valley located between the Central Mountain Range and the Coastal Mountain Range. Most of the rising surface temperatures rates are accelerating. As a result, this situation provides the effect of urbanization and agriculture activities clearer and offers policymakers a stiff warning for better planning and managing in reaction to increased global warming.

Even though the coverage of the greenness rates is not lowered yet, a sensible plan is required to retain pace with the accelerating temperature conditions.

Furthermore, this analysis illustrated a practical and effective method to statistical modeling of daytime LST and NDVI for spatial and temporal variations based on MODIS time-series data for the last 20 years over Taiwan Island. This methodology provides us with the opportunity to discover what is happening at a sub-region level and at the smallest area of 1 km. The study found that there were with statistical conclusions, not exploratory analysis. In addition, ground surface temperature and vegetation index trends were investigated by using the natural cubic spline function with annual periodic boundary conditions. Moreover, their acceleration rates were highlighted using the multivariate regression model analysis. The approaches used in this analysis could be applied in another regions and locations.

Furthermore, this study demonstrated the use of a linear model with weight some contrast for adjusting each determinate factor to assess the influence of LC variation and elevation on a decadal trend of LST in Taiwan. It is an example of diverse terrain with a high mountain range, gorges and sharp valleys and the flat to gently rolling plains, where 90% of the population lives. LC in Taiwan had changed only 9.81% of the whole island in the last two decades, and the majority of the transformed areas were found in the land that its elevation was around 90.5 m by median. This raises awareness when it comes to analyzing and compares the average LST change in different groups of LC change and level of elevation as the factors of determinant that could have a significant difference in sample size and influence each other. The presented method can compare several means with comparative confidence intervals based on weighted sum contrasts, which are often more appropriate than those based on treatment contrasts needing specify a control group. The results reveal that the average daytime LST trends were 0.14 °C/decade while the average of nighttime LST trends was 0.31 °C/decade. The difference in LC change does not affect nighttime LST trends. However, the mean of daytime LST in urban, built-up and barren areas shows a significantly different overall mean. The effect of LC and elevation differed according to the difference in geography and sub-region. There was an effect of high elevation (> 600 m) in both daytime and nighttime LSTs. The area above 600 to 2000 m of elevation in Taiwan with their surface temperature trends to increase is worth investigating. Changing of LC, elevation, NDVI and other factors influencing the increase in LST for example LU, precipitation and air temperature should be investigated in other different geographical areas in further studies using the presented method.

4.3 Limitation and recommendation for further study

This research was used the cubic spline model to investigate the seasonal patterns and trends of LST and NDVI. Further studies should be applied different methods to model the seasonal patterns and trends of LST and NDVI variation. Moreover, the cubic spline model with 0 and 4 knots was applied to examine LST and NDVI change. Further research could use the different numbers of the placement knot to investigate the result. In addition, the Pearson correlation was used to investigate the correlation between LST and NDVI change across five major LC classes. Further study could applied another correlation coefficient method to investigate the correlation between those variables.

The surface temperature and vegetation index variation at Taiwan’s local level is necessary for policymakers to observe for better control of undesirable consequences.

Moreover, the government or related parties have to find the best solutions for a proper formulation of policies before beginning any developmental, social, and economic activities. Moreover, this study has to apply other methods, for example, machine learning methods to compare with the performance of the statistical methods in climate variation. Finally, further studies have to consider more factors in order to analyze which factors that have a high impact on the change of the surface temperature.

References

Aboelnour, M. and Engel, B. 2018. Application of remote sensing techniques and geographic information systems to analyze land surface temperature in response to land use/land cover change in greater Cairo region, Egypt. Journal of Geographic Information System, 10(1), 57-88.

Agyakwah, W. and Lin, Y.L. 2021. Generation and enhancement mechanisms for extreme orographic rainfall associated with Typhoon Morakot (2009) over the central mountain range of Taiwan. Atmospheric Research. 247, 105160.

Beardsmore, G.R. 2005. High-resolution heat-flow measurements in the southernCarnarvon Basin, Western Australia. Exploration Geophysics. 36 (2), 206–215.

Bounoua, L., Collatz G.J., Los S.O., Sellers P.J., Dazlich D.A., Tucker C.J., and Randall D.A. 2000. Sensitivity of climate to changes in NDVI. Journal of Climate.13: 2277-229.

Cai, H., Liu, P., Song, J.B. and Zeng, Z.Z. 2011. Study on retrieval of urban heat island effect from RS date in a typical karst area–A case study in Guiyang city. Earth & Environment 39, 246–250.

Cai, Y., Zhang, H., Zheng, P. and Pan, W. 2016. Quantifying the impact of land use/land cover changes on the urban heat island: A case study of the natural wetlands distribution area of Fuzhou city, China. Wetlands. 36, 285–298.

Casella G. 2008. Statistical design. Springer. Springer Science & Business Media. ISBN 978-0-387-75965-4.

Feng, G. 1998. Data smoothing by cubic spline filters. IEEE Transaction on Signal Processing, 46, 2790–2796.

Chandola, V., Hui, D., Gu, L., Bhaduri, B. and Vatsavai, R.R. 2010. Using time series segmentation for deriving vegetation phenology indices from MODIS NDVI data. In 2010 IEEE International Conference on Data Mining Workshops (pp. 202-208). IEEE.

Charlie, J. Tomlinson, Lee, C., Thornesb, J.E. and Bakera, C. 2011. Remote sensing land surface temperature for meteorology and climatology. Meteorological Application 296-306. Doi: 10.1002/met.287

Chen, M., Zhou, Y., Hu, M. and Zhou, Y. 2020. Influence of urban scale and urban expansion on the urban heat island effect in metropolitan areas: Case study of Beijing–Tianjin–Hebei urban agglomeration. Remote Sensing. 12(21), 3491.

Chen, W., Chang, M., Chen, J., Lu, W., Huang, C.C. and Wang, Y. 2013. The warming trend of ground surface temperature in the Choshui Alluvial Fan, western central Taiwan. In AGU Fall Meeting Abstracts (Vol. 2013, pp. EP13C-0882).

Chen, S.T., Lai, Y.J. and Wang, Y.C. 2016. Effects of urban heat island and increased temperature on convective rainfall in Taichung city. Taiwan Water Conservancy. 64(3), 13-22.

Chen, Y.C., Lin, T.P. and Lin, C.T. 2017. A simple approach for the development of urban climatic maps based on the urban characteristics in Tainan, Taiwan. International Journal of Biometeorology. 61(6), 1029-1041.

Chiang, J.L. and Liu, T.M. 2013. Impact of climate change on paddy field irrigation in southern Taiwan. Paddy and Water Environment. 11(1), 311-320.

Chien, F.C. and Kuo, H.C. 2011. On the extreme rainfall of Typhoon Morakot (2009). Journal of Geophysical Research: Atmospheres. 116(D5).

Devi, R.M., Prasetya, T.A.E. and Indriani, D. 2021. Spatial and temporal analysis of land surface temperature change on New Britain Island. International Journal of Remote Sensing and Earth Sciences. 17(1), 45-56.

Dislich, C., Keyel, A.C., Salecker, J., Kisel, Y., Meyer, K.M., Auliya, M., Barnes, A.D., Corre, M.D., Darras, K., Faust, H., Hess, B., Klasen, S., Knohl, A., Kreft, H., Meijide, A., Nurdiansyah, F., Otten, F., Pe'er, G., Steinebach, S., Tarigan, S., Tölle, M.H., Tscharntke, T. and Wiegand, K. 2016. A review of the ecosystem functions in oil palm plantations, using forests as a reference system, Biological Reviews, 92, 1539-1569.

Du, J., Song, K. and Yan, B. 2019. Impact of the Zhalong wetland on neighboring land surface temperature based on remote sensing and GIS. Chinese Geographical Science. 29, 798–808.

Estoque, R.C., Murayama, Y. and Myint, S.W. 2017. Effects of landscape composition and pattern on land surface temperature: An urban heat island study in the megacities of Southeast Asia. Science of the Total Environment, 577, 349–359.

Feehan, J., Harley, M. and Minnen, J.V. 2009. Climate change in Europe. 1. Impact on terrestrial ecosystem and biodioversity: A review. Agronomy for Sustainable Development, 29, 409-421.

Fitrahanjani, C., Prasetya, T.A.E. and Indawati, R.A. 2021. Statistical method for analysing temperature increase from remote sensing data with application to Spitsbergen Island. Modeling Earth Systems and Environment. 7, 561–569.

Ghobadi, Y., Pradhan, B., Shafri, H.Z.M. and Kabiri, K. 2014. Assessment of spatial relationship between land surface temperature and land use/cover retrieval from multi-temporal remote sensing data in South Karkheh Sub-basin, Iran. Arabian Journal of Geosciences 8, 525–537.

Guha, S., Govil, H., Dey, A. and Gill, N. 2018. Analytical study of land surface temperature with NDVI and NDBI using Landsat 8 OLI and TIRS data in Florence and Naples city, Italy. European Journal of Remote Sensing. 51(1), 667-678.

Guha, S. and Govil, H. 2020. An assessment on the relationship between land surface temperature and normalized difference vegetation index. Environment, Development and Sustainability. 1-20.

Guo, Z., Wang, S. D., Cheng, M.M. and Shu, Y. 2012. Assess the effect of different degrees of urbanization on land surface temperature using remote sensing images. Procedia Environmental Sciences, 13, 935-942.

Hamoodi, M.N., Corner, R. and Dewan, A. 2019. Thermophysical behaviour of LULC surfaces and their effect on the urban thermal environment. Journal of Spatial Science. 64(1), 111-130.

Hansen, P.M. and Schjoerring, J.K. 2003. Reflectance measurement of canopy biomass and nitrogen status in wheat crops using normalized difference vegetation indices and partial least squares regression. Remote Sensing of Environment, 86, 542-553.

He, G., Zhen, X., Li, Z., Shen, W., Han, J., Zhang, L. and Zhang, R. 2020. Influence of variations of hydrothermal conditions on NDVI in typical temperature zones along the East Coast of China. Frontiers in Earth Science. 8, 394.

Hou, G.L., Zhang, H.Y., Wang, Y.Q., Qiao, Z.H. and Zhang, Z.X. 2010. Retrieval and spatial distribution of land surface temperature in the middle part of jilin province aased on MODIS data. Scientia Geographica Sinica 30, 421–427.

Hsu, H.H. and Chen, C.T. 2002. Observed and projected climate change in Taiwan. Meteorology and Atmospheric Physics. 79(1-2), 87-104.

Huang, J.M. and Chen, L.C. 2020. A numerical study on mitigation strategies of urban heat islands in a tropical megacity: A case study in Kaohsiung City, Taiwan. Sustainability 12(10), 3952.

Huryan, H., Brom, J. and Pokorny, J. 2014. The importance of wetlands in the energy balance of an agricultural landscape. Wetlands Ecology and Management. 22(4):363-381.

Hung, T., Uchihama, D., Ochi, S. and Yasuoka, Y. 2006. Assessment with satellite data of the urban heat island effects in Asian mega cities. International Journal of Applied Earth Observation and Geoinformation, 8(1), 34-48.

Huang, T.C. and Hsieh, C.F. 1994−2003. Flora of Taiwan, Vol. 1−6, 2nd ed. National Taiwan University, Taipei, TW.

Imhoff, M., Zhang, P., Wolfe, R. and Bounoua, L. 2010. Remote sensing of the urban heat island effect across biomes in the continental USA. Remote Sensing of Environment, 114, 504–513.

Imran, H.M., Kala, J., Ng, A.W. and Muthukumaran, S. 2019. Impacts of future urban expansion on urban heat island effects during heat wave events in the city of Melbourne in southeast Australia. Quarterly Journal of the Royal Meteorological Society. 145(723), 2586-2602.

Islam, S. and Ma, M. 2018. Geospatial monitoring of land surface temperature effects on vegetation dynamics in the southeastern region of Bangladesh from 2001 to 2016. ISPRS International Journal of Geo-Information. 7(12), 486.

Ismail, N.A., Zin, W.Z.W., Ibrahim, W. and Yeun, L.C. 2019. Eight-day daytime land surface temperature pattern over peninsular Malaysia. International Journal of Technology and Engineering. 8, 11949-11955.

Jia, Q., Zhou, L., Yu, W., Wang, X., Wen, R. and Xie, Y. 2020. Surface energy flux changes and budget in a typical coastal reed wetland (Liaohe Delta, China). Journal of Coastal Research. 36(5):1005-1012.

Jin, M., Dickinson, R. and Zhang, D. 2005. The footprint of urban areas on global climate as characterized by MODIS. Journal of Climate, 18, 1551–1565.

Johannessen, O.M., Bengtsson, L., Miles, M.W., Kuzmina, S.I., Semenov, V.A. and Alekseev, G.V. 2004. Arctic climate change: Observe and modeled temperature and sea-ice variability. Tellus, 56, 328-341.

Julien, Y., Sobrino, J.A. and Verhoef, W. 2006. Changes in land surface temperatures and NDVI values over Europe between 1982 and 1999. Remote Sensing of Environment, 103, 43–55.

Karnieli, A., Agam, N., Pinker, R.T., Anderson, M., Imhoff, M.L., Gutman, G.G. and Panov, N. 2010. Use of NDVI and land surface temperature for drought Assessment: merits and limitations. Journal of Climate, 23, 618-633.

Kato, S., Liu, C.C., Sun, C.Y., Chen, P.L., Tsai, H.Y. and Yamaguchi, Y. 2012. Comparison of surface heat balance in three cities in Taiwan using Terra ASTER and Formosat-2 RSI data. International Journal of Applied Earth Observation and Geoinformation. 18, 263-273.

Khandelwal, S., Goyal, R., Kaul, N. and Mathew, A. 2018. Assessment of land surface temperature variation due to change in elevation of area surrounding Jaipur, India. The Egyptian Journal of Remote Sensing and Space Sciences 21 (2018) 87–94.

Kong, D., Zhang, Q., Singh, V.P. and Shi, P. 2017. Seasonal vegetation response to climate change in the Northern Hemisphere (1982–2013). Global and Planetary Change. 148, 1-8.

Kumar, D. and Shekhar, S. 2015. Statistical analysis of land surface temperature–vegetation indexes relationship through thermal remote sensing. Ecotoxicology and Environmental Safety. 121, 39-44.

Kumar, K.S., Bhaskar, P.U. and Padmakumari, K. 2012. Estimation of land surface temperature to study urban heat island effect using LANDSAT ETM+ image. International Journal of Engineering, Science and Technology. 4 (2), 771–778.

Lean, .L. and Rind, .H. 2009. How will earth's surface temperature change in future decades? Geophysical Research Letters. 36, L15708. Doi:10.1029 /2009GL038932.

Lee, Y.J., Tung, C.M., Lee, P.R. and Lin, S.C. 2016. Personal water footprint in Taiwan: A case study of Yunlin County. Sustainability. 8(11), 1112.

Lin, C.Y., Chen, F., Huang, J.C., Chen, W.C., Liou, Y.A., Chen, W.N. and Liu, S.C. 2008. Urban heat island effect and its impact on boundary layer development and land–sea circulation over northern Taiwan. Atmospheric Environment. 42(22), 5635-5649.

Liu, F., Zhang, Z. and Wang, X. 2016. Forms of urban expansion of Chinese municipalities and provincial capitals, 1970s–2013. Remote Sensing. 8(11), 930.

Li, W.F., Cao, Q.W., Kun, L. and Wu, J.S. 2017. Linking potential heat source and sink to urban heat island: Heterogeneous effects of landscape pattern on land surface temperature. Science of the Total Environment, 586, 457–465.

Liu, Y., Li, Y., Li, S. and Motesharrei, S. 2015. Spatial and temporal patterns of global NDVI trends: Correlations with climate and human factors. Remote Sensing, 7(10), 13233-13250.

Liu, Y., Hiyama, T. and Yamaguchi, Y. 2006. Scaling of land surface temperature using satellite data: A case examination on ASTER and MODIS products over a heterogeneous terrain area. Remote Sensing of Environment, 105, 115–128.

Mao, F., Li, X., Du, H., Zhou, G., Han, N., Xu, X., Liu, Y., Chen, L. and Cui, L. 2017. Comparison of two data assimilation methods for improving MODIS LAI time series for bamboo forests. Remote Sensing, 9(5), 401.

McNeil, N. and Chooprateep, S. 2014. Modeling sea surface temperatures of the North Atlantic ocean. Theoretical and Applied Climatology, 116, 11–17.

McNeil, N. and Wanishsakpong, W. 2012. Modelling of daily maximum temperatures over Australia from 1970 to 2012. Meteorological Application, 23, 115–122.

Muro, J., Strauch, A., Heinemann, S., Steinbach, S., Thonfeld, F., Waske, B. and Diekkrüger, B. 2018. Land surface temperature trends as indicator of land use changes in wetlands. International Journal of Applied Earth Observation and Geoinformation. 70, 62-71.

National Geography 2019. Elevation. https://www.nationalgeographic.org/encyclopedia/elevation. Accessed 19 March 2019

Neteler, M. 2010. Estimating daily land surface temperatures in mountainous environments by reconstructed MODIS LST Data. Remote Sensing, 2, 333–351.

ORNL DAAC 2018. MODIS and VIIRS land products global subsetting and visualization tool. ORNL DAAC, Oak Ridge, Tennessee, USA. https://doi.org/10.3334/ORNLDAAC/1379. Accessed 11 March 2021

Pan, T. 2016. Variation of land surface temperature of Harbin city based landsat TM Data in 2001–2015. Scientia Geographica Sinica, 36, 1759–1766.

Pepin, N., Deng, H., Zhang, H., Zhang, F., Kang, S. and Yao, T. 2019. An examination of temperature trends at high elevations across the Tibetan Plateau: The use of MODIS LST to understand patterns of elevation-dependent warming. Journal of Geophysical Research: Atmospheres, 124(11), 5738-5756.

Phan, T., Kappas, M. and Tran, T. 2018. Land surface temperature variation due to changes in elevation in northwest Vietnam. Climate, 6(2), 28.

Piao, S., Fang, J., Zhou, L., Guo, Q., Henderson, M., Ji, W. and Tao, S. 2003. Interannual variations of monthly and seasonal normalized difference vegetation index (NDVI) in China from 1982 to 1999. Journal of Geophysical Research: Atmospheres. 108(D14).

Pongr´acz R, Bartholy J and Dezs¨o Z. 2010. Application of remotely sensed thermal information to urban climatology of Central European cities. Physics and Chemistry of the Earth 35, 95–99.

Pourhoseingholi, M.A., Baghestani, A.R. and Vahedi, M. 2012. How to control confounding effects by statistical analysis. Gastroenterology and hepatology from bed to bench, 5(2), 79.

Prasetya, T.A.E., Munawar, M., Taufik, M.R., Chesoh, S., Lim, A. and McNeil, D. 2020. Land surface temperature assessment in Central Sumatra, Indonesia. Indonesian Journal of Geography. 52(2), 227-238.

Przyborski, P. 2019. Measuring vegetation (NDVI and EVI). Retried on 6/2/19 from https://earthobservatory.nasa.gov/features/MeasuringVegetation/measuring_vegetation_2.php

Qiao, Z., Tian, G., Zhang, L. and Xu, X. 2014. Influences of urban expansion on urban heat island in Beijing during 1989–2010. Advances in Meteorology. 2014, 187169.

Qu, C., Ma, J.H., Xia, Y.Q. and Fei, T. 2014. Spatial distribution of land surface temperature retrieved from MODIS data in Shiyang River Basin. Arid Land Geography, 37, 125–133.

R Core Team 2020. A language and environment for statistical computing, R Foundation for Statistical Computing, Vienna, Austria.

Ro-Ting, L. and Chang-Chuan, C. 2009. Effects of heat on workers' health and productivity in Taiwan. Global Health Action, 2, 10.3402. Available online: https://www.ncbi.nlm.nih.gov/pmc/articles/PMC2799321

Semenov, V.A. 2007. Structure of temperature variability in the high latitudes of the northern hemisphere. Atmospheric and Oceanic Physics, 43(6), 687-695.

Sharma, I., Tongkumchum, P. and Ueranantasun, A. 2018a. Modeling of land surface temperatures to determine temperature patterns and detect their association with altitude in the Kathmandu Valley of Nepal. Chiang Mai University Journal of Natural Sciences. 17(4).

Sharma, I., Ueranantasun, A. and Tongkumchum, P. 2018b. Modeling of satellite data to identify the seasonal patterns and trends of vegetation index in Kathmandu Valley, Nepal from 2000 to 2015. The Journal of Technology, 80(4).

Shigeto, K. 1994. Relation between vegetation, surface temperature, and surface composition in the Tokyo region during winter. Remote Sensing of Environment 50, 52–60.

Shih, W.Y., Ahmad, S., Chen, Y.C., Lin, T.P. and Mabon, L. 2020. Spatial relationship between land development pattern and intra-urban thermal variations in Taipei. Sustainable Cities and Society. 62, 102415.

Smith, R.C.G. and Choudhury, B.J. 1990. On the correlation of indices of vegetation and surface temperature over south-eastern Australia. International Journal of Remote Sensing, 11, 2113–2120.

Stroppiana, D., Antoninetti, M. and Brivio, P.A. 2014. Seasonality of MODIS LST over Southern Italy and correlation with land cover, topography and solar radiation. European Journal of Remote Sensing, 47, 133–152.

Tan, C.H. 2007. Effects of temperature variation induced and economic assessment from paddy cultivation, (in Chinese). Presented at Agricultural Engineering Research Center, Chungli, Taiwan.

Tomlinson, C.J., Chapman, L., Thrones, J.E. and Baker, C. 2011. Remote sensing land surface temperature for meteorology and climatology: a review. Meteorological Applications, 18, 296–306.

Tongkumchum, P. and McNeil, D. 2009. Confidence intervals using contrasts for regression model. Songklanakarin Journal of Science and Technology, 31(2).

Tsai, H. P. and Yang, M. D. 2016. Relating vegetation dynamics to climate variables in Taiwan using 1982–2012 NDVI3g data. IEEE Journal of Selected Topics in Applied Earth Observations and Remote Sensing. 9(4), 1624-1639.

Tsou, C.Y., Feng, Z.Y. and Chigira, M. 2011. Catastrophic landslide induced by typhoon Morakot, Shiaolin, Taiwan. Geomorphology. 127(3-4), 166-178.

Tulu H.D., Lim A., Ma-a-Lee A., Bundhamcharoen K. and Makka N. 2020. Prediction of HIV mortality in Thailand using three data sets from the national AIDS program database. Sains Malaysiana 49(1), 155-160.

Ullah, S., Tahir, A.A., Akbar, T.A., Hassan, Q.K., Dewan, A., Khan, A.J. and Khan, M. 2019. Remote sensing-based quantification of the relationships between land use land cover changes and surface temperature over the Lower Himalayan Region. Sustainability. 11(19), 5492.

Vadasz, V. 1994. On the relationship between surface temperature, air temperature and vegetation index. Advances in Space Research, 14(3), 41-44.

Wang, Y.P., Chen, C.T., Tsai, Y.C. and Shen, Y. 2021. A sentinel-2 image-based irrigation advisory service: Cases for tea plantations. Water. 13(9), 1305.

Wanishsakpong, W. and McNeil, N. 2016. Modelling of daily maximum temperatures over Australia from 1970 to 2012. Meteorological Applications, 23(1), 115-122.

Wen, L.J. 2017. Ananalysis of land surface temperature (LST) and its influencing factors in summer in western Sichuan Plateau: A case study of Xichang City. Remote Sensing for Land and Resources, 29, 207–214.

Wongsai, N., Wongsai, S. and Huete, A.R. 2017. Annual seasonality extraction using the cubic spline function and decadal trend in temporal daytime MODIS LST data. Remote sensing, 9, 1254.

Wongsai, N., Wongsai, S., Lim, A., McNeil, D. and Huete A.R. 2020a. Impacts of spatial heterogeneity patterns on long-term trends of Moderate Resolution Imaging Spectroradiometer (MODIS) land surface temperature time series. Journal of Applied Remote Sensing. 14(1), 014513.

Wongsai N., Wongsai S., Lim A., McNeil D. and Huete A.R. 2020b. Statistical model for land surface temperature change over mainland Southeast Asia. International Journal of Geoinformatics 16(2).

World Population Review 2019. Population of cities in Taiwan 2019. Retrieved on 7/2/2019 from http://worldpopulationreview.com/countries/taiwan-population/cities

Wu, C. C. 2013. Typhoon Morakot: key findings from the journal TAO for improving prediction of extreme rains at landfall. Bulletin of the American Meteorological Society, 94(2), 155-160.

Xu, C., Liu, M., Zhang, C., An, S., Yu, W. and Chen, J.M. 2007. The spatiotemporal dynamics of rapid urban growth in the Nanjing metropolitan region of China. Landscape Ecology. 22, 925-937.

Yang, S.Y., Jan, C.D. and Wang, J. S. 2018. Landslides triggered by typhoon Morakot in Taiwan, in: Mihai, F.C., Grozavu, A. (Eds.), Environmental Risks, IntechOpen, London.

Yuan, X.L. 2017. Vegetation changes and land surface feedbacks drive shifts in local temperatures over Central Asia. Scientific Report, 7, 3287, https://doi.org/10.1038/s41598017034322

Yuanhong, D., Shijie, W., Xiaoyong, B., Yichao, T., Luhua, W., Jianyong, X., Fei, C. and Qinghuan, Q. 2018. Relationship among land surface temperature and LUCC, NDVI in typical karst area. Scientific Report, 8, 641. Doi: 10.1038/s41598-017-19088-x

Ye, J.-S., Reynolds, J.F., Maestre, F.T. and Li, F.-M. 2016. Hydrological and ecological responses of ecosystems to extreme precipitation regimes: a test of empirical-based hypotheses with an ecosystem model. Perspectives in Plant Ecology, Evolution and Systematics. 22, 36-46.

Yue, W.Z., Hua, X.J. and Hua, X.L. 2006. An analysis on eco-environmental effect of urban land use based on remote sensing images: a case study of urban thermal environment and NDVI. Acta Ecologica Sinica, 26, 1450–1460.

Yue, W., Xu, J., Tan, W. and Xu, L. 2007. The relationship between land surface temperature and NDVI with remote sensing: application to Shanghai Landsat 7 ETM+ data. International Journal of Remote Sensing. 28(15), 3205-3226.

Zhang, X., FRriedl, M.A., Schaaf, C.B., Strahler, A.H., Hodges, J.C.F., Gao, F., Reed, B.C. and Huete, A. 2003. Monitoring vegetation phenology using MODIS. Remote Sensing of Environment, 84(3), 471-475.

Zhao, M., Cai, H., Qiao, Z. and Xu, X. 2016. Influence of urban expansion on the urban heat island effect in Shanghai. International Journal of Geographical Information Science. 30(12), 2421-2441.

Appendix

Remote Sensing Applications: Society and Environment 24 (2021) 100636

Contents lists available at ScienceDirect

Remote Sensing Applications: Society and Environment

journal homepage: www.elsevier.com/locate/rsase

Land surface temperature and vegetation cover changes and their relationships in Taiwan from 2000 to 2020

Sahidan Abdulmana [a], Apiradee Lim, Ph.D. [a,b,*], Sangdao Wongsai [c,d], Noppachai Wongsai [d]

[a] Department of Mathematics and Computer Science, Faculty of Science and Technology, Prince of Songkla University, Pattani, 94000, Thailand
[b] Air Pollution and Health Effect Research Center, Prince of Songkla University, Hat Yai, Songkhla, 90110, Thailand
[c] Department of Mathematics and Statistics, Faculty of Science and Technology Thammasat University, Pathumthani, 12121, Thailand
[d] Thammasat University Research Unit in Data Learning, Thammasat University, Pathumthani, 12121, Thailand

ARTICLE INFO

Keywords:
Subtropical island
Land surface warming
NDVI
Cubic spline function
Time series analysis
Multivariate regression model

ABSTRACT

This study reported decadal trends and acceleration patterns of surface temperatures and vegetation conditions in Taiwan from 2000 to 2020. Time series data on Land Surface Temperature (LST), Normalized Difference Vegetation Index (NDVI), and Land Cover (LC) types were obtained from the Moderate Resolution Imaging Spectroradiometer (MODIS) sensor. Seasonal patterns, decadal trends, and acceleration rates for each LU type were evaluated using the natural cubic spline method and multivariate linear regression. Acceleration patterns were then analyzed using the correlations between derived trends and acceleration rates. Results are provided for the entire island, for sub-regions, and for the smallest area elements of 1 km^2. Taiwan has had a significant mean increase in decadal trends of NDVI (95%CI: 0.013–0.025 unit/dec), but not of LST (95%CI: −0.018-0.302 °C/dec). Negative correlation between LST and NDVI was stronger in green coverage areas than in built-up areas. On sub-regional level, a larger increase in surface temperature and tremendous vegetation loss were observed at high elevations in the southern regions of the Central Mountain Range. Meanwhile, the central-western lowlands faced moderately warming temperatures and slight greening. At the pixel level, urbanization and agricultural expansion have caused rising surface temperatures, while afforestation contributes cooling. The rise in temperature in accelerating in the different LC types throughout Taiwan. Despite that, the acceleration patterns of the vegetation index have remained stable in most parts of the island. Although the rates of vegetation growth have not yet declined, practitioners and policymakers need to consider a balanced view of green cities to keep pace with the accelerating temperature conditions.

1. Introduction

Land Surface Temperature (LST) is an important parameter in local and global climate change. It has greatly affected the natural environment and human society (Song et al., 2018). LST has risen in several parts of the world (Prasetya et al., 2020). The increase in LST is due to anthropogenic heat release caused by energy consumption and correlated to a decrease in vegetation cover (Kumar et al., 2012). Normalized Difference Vegetation Index (NDVI) is a plant health index of greenness on land that can be used to analyze the density of vegetation on the ground. Vegetation changes are large-scale in transformations that lead to significant losses in plant diversity, animals, and ecosystem functions, and changes in microclimate conditions (Dislich et al., 2016). In the current global environment, a decline in NDVI has resulted from rapid urbanization, construction and deforestation that increase LST (Ullah et al., 2019; Yuen and Kong, 2009). Land use and land cover changes, especially urban expansion, are key factors affecting trends and patterns in LST and NDVI (Kafy et al., 2021).

Moderate Resolution Imaging Spectroradiometer (MODIS) satellites deliver various data products with different spatial and temporal resolutions that are important for regional evaluation of LST and NDVI distributions (Haq et al., 2020). From publicly available MODIS data, relations between LST and NDVI have been established in previous studies, including in the northern and southern Hemisphere with the Brazilian plateau, Pampas steppe, southeastern Africa, and Australia (Song et al., 2018), northern India (Haq et al., 2020), and southeastern

* Corresponding author. Department of Mathematics and Computer Science, Faculty of Science and Technology, Prince of Songkla University, Pattani, 94000, Thailand.
E-mail address: apiradee.s@psu.ac.th (A. Lim).

https://doi.org/10.1016/j.rsase.2021.100636
Received 11 May 2021; Received in revised form 21 September 2021; Accepted 22 September 2021
Available online 24 September 2021
2352-9385/

Manuscript Submitted	27.09.2021
Accepted	23.12.2021
Published	31.12.2021

Modeling Vegetation Index Changes in Taiwan from 2000 to 2020

Sahidan Abdulmana & Apiradee Lim
Faculty of Science and Technology
Prince of Songkla University
yee_laal@hotmail.com

Ibtisam Hama
Faculty of Science and Technology
Fatoni University
ibtisam_alhamadi@ftu.ac.th

Abstract

Vegetation changes play an important roles in climate change. Information from patterns and trends of these factor reveals the state of the climate in a particular area and can be used to set up a proper monitoring program. This study aimed to investigate the annual seasonal patterns and trends of Normalized Difference Vegetation Index (NDVI) by sub-region and by region and to estimate NDVI increase per decade by region in Taiwan. NDVI time series data from 2000 to 2020 were downloaded from the MODIS website. The natural cubic spline method was used to model NDVI annual seasonal patterns and linear regression was used to investigate the trends. Furthermore, multivariate regression was applied to adjust spatial correlation and to estimate NDVI increases in each sub-region and region. The results show the NDVI increase in March of sub-region 1, 2, 3, 4, and 7 and sub-region 3 and 6 show two peaks in each year. The trends show sub-region 8 in region 1 had the highest mean NDVI which was above 0.8, while sub-region 2 had the lowest mean NDVI which was below 0.4. However, NDVI shows increasing trend in almost sub-region except sub-region 15, 22, 23, 27 and 36. In addition, the NDVI in all regions had increasing trends, except in the eastern Taiwan with stable trend. The average increased of NDVI was 0.01 per decade. In conclusion, vegetation index in Taiwan is considerably increasing while the causes of the increasing trends need to be examined in further studies.

Keywords: *Normalized difference vegetation index, cubic spline function, multivariate regression model*

1. Introduction

Normalized Difference Vegetation Index (NDVI) is a plant health index of greenness on land that can be used to analyze the density of vegetation on the ground. Vegetation is one significant to the energy balances on regional and global scales (Huryna & Pokorný, 2016). Furthermore, vegetation absorbs carbon dioxide during the day and releases oxygen to the ecosystem and for human beings. Alterations of vegetation can be assessed at various wavelengths in the visible and near infrared ranges, in which the flora reflects sunlight. Plant leaves tend to reflected a wide range of light wavelengths (Przyborski, 2019).

Vegetation changes not only interrupt carbon dioxide and water cycle, but also influence energy balance of the Earth's surface, and affect LST changes (Liu et al., 2015). The alterations of vegetation on the ground from short to long term influence climate change at local and global scales (Bounoua, Collatz, Los, Sellers, Dazlich, Tucker & Randall, 2000). Increasing deforestation and human population affect the climate change especially reduction of greenness. Increasing NDVI has been

Modeling for seasonal pattern and trend of land surface temperature in Taiwan

Sahidan Abdulmana, Apiradee Lim
Department of Mathematics and Computer Science, Faculty of Science and Technology, Prince of Songkla University, Pattani, Thailand

Abstract:
Land surface temperature (LST) is one of the most significant factors of surface atmospheric interaction. It is dramatically changed on an adequate distribution and temporal evolution in time and space. Moreover, LST might change the pattern from natural disaster in such cases of landslide, forest fire and rainfall. This study focused in Taiwan which lies in northern tropic of cancer and circles on earth at which the sun can be directly overhead. The aim of this study was to examine the seasonal pattern and trend of average increase in LST in Taiwan. The data was downloaded from Terra eight-day MODIS land surface temperature product have ~ 1km2 pixels with 18 years. The natural cubic spline was used to extract annual LST seasonal pattern without checking to estimate the missing values. The result of this study showed that the significant of using cubic spline was an appropriate number of the knots which was eight knots. The seasonal patterns of different sub-regions in the same region had similar patterns. In addition, there was a steady increase of LST in June and the peak was in summer which was in July. From August, it was rapidly declined and reached the lowest point in winter during December and January. The trend indicated accelerate decrease in some regions at northern part of Taiwan but, the northern and central part of Taiwan the trend is accelerate increase in most regions.

Keywords
Land surface temperature; temperature pattern; trend analysis; natural cubic spline

1. Introduction

The temperature of the land surface skin is known as Land Surface Temperature (LST). Its could be measured at the interface between surface materials such as roof of building, grass, snow, ice, water, soil, top of plant and the atmosphere. LST is the hot or warm of the ground surface in the world would feel to the touch in a particular location. LST is being increasingly recognized and interested in developing methodologies to measure temperature change from surface. Scientists monitor LST because the warmth rising off world's surface effects our world's climate patterns and weather. Moreover, they need to screen how growing land surface temperatures

การประเมินการเปลี่ยนแปลงอุณหภูมิพื้นผิวในไต้หวันตั้งแต่ปี 2000-2020

Assessment of land surface temperature changes in Taiwan from 2000 to 2020

Sahidan Abdulmana[1], Apiradee Saelim[1]

[1] Department of Mathematics and Computer Science, Faculty of Science and Technology, Prince of Songkla University, Pattani Campus

Abstract

Land Surface Temperature (LST) changes play important roles in climate change. This study aimed to investigate the annual seasonal patterns and trends of LST by sub-region and by region. Daytime LST time series data from 2000 to 2020 was downloaded from the MODIS website. The natural cubic spline method was used to model daytime LST annual seasonal patterns and linear regression was used to investigate the trends. Furthermore, multivariate regression was applied to adjust spatial correlation and to estimate daytime LST increases in each sub-region and region. The results show that daytime LST in Taiwan has increased on average by 0.1 °C per decade. Most of the daytime LST by sub-region were stable. Furthermore, daytime LST in all regions had increasing trends, except in the eastern Taiwan with stable trend. In conclusion, daytime LST in Taiwan is gradually increasing. The causes of the increasing trends of LST need to be examined in further studies.

Introduction

Land Surface Temperature (LST) is the ground temperature of the earth's surface resulting from land surface-atmosphere interactions and energy fluxes between the surface and the atmosphere (Khandelwal et al. 2018). The urbanization has increased rapidly since 1967. The expansion of population in Taiwan has influenced temperature changes (Lai and Cheng, 2010). Therefore, this study aimed to investigate daytime LST seasonal patterns and trends in Taiwan from 2000 to 2020.

Methods

The natural cubic spline method with are eight knots assigned in this model, which were on the days 10, 40, 80, 130, 240, 290, 330 and 360 was used to model daytime LST annual seasonal patterns. Linear regression was used to investigate the LST trends. In addition, to eliminate spatial correlation, the average increases of daytime LST by region were estimated by using multivariate regression model.

Acknowledgement

We would like to thank the Royal Golden Jubilee Ph.D. program Scholarship under Thailand Science Research and Innovation (TSRI) and National Research Council of Thailand (NRCT) (Grant No. PHD/0205/2560). We acknowledge the Department of Research Methodology, Prince of Songkla University, Pattani campus, for providing facilities for this study. We are grateful to Professor Don McNeil for his immense guidance during the study.

Results

Daytime LST seasonal adjusted

Daytime LST changes by sub-region and region

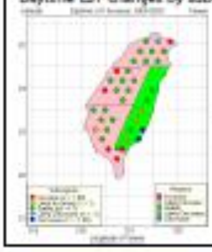

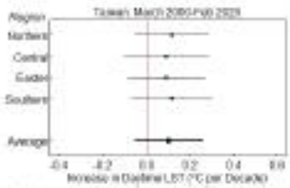

Daytime LST increases per decade from 2000 to 2020

Conclusion

This study showed that cubic spline method with an appropriate number of knots and linear regression could successfully extract annual daytime LST seasonal patterns and trends. The average increase of daytime LST was 0.1 °C per decade. Our study supports the result from the Council for Economic Planning and Development in Taiwan, which reported that Taiwan's annual temperature had increased by 0.29 °C per decade (1980-2009) (Council for Economic Planning and Development, 2012). The study found that daytime LST in Taiwan have increased in the last two decades. The increase in daytime LST is due to the rapid growth of Taiwan's economy and its industrialization, which have increased energy consumption. The climate and spatial changes are terrible threats to ecosystems. Therefore, this is a signal to the Taiwanese policy makers to campaign against global warming.

References

Khandelwal, S., Goyal, R., Kaul, N., & Mathew, A. (2018). Assessment of land surface temperature variation due to change in elevation of area surrounding Jaipur, India. The Egyptian Journal of Remote Sensing and Space Sciences, 21, (2018) 87-94.

Impact of Elevation and Land Cover on Land Surface Temperature Seasonal Patterns and Trends in Taiwan from 2000 - 2020

Sahidan Abdulmana[1], Apiradee Lim[1]

[1]Department of Mathematics and Computer Science, Faculty of Science and Technology, Prince of Songkla University, Pattani Campus

Abstract

This study aimed to investigate the seasonal patterns and trends of daytime LST and to examine the impact of elevation and LC on daytime LST in Taiwan from 2000 to 2020. LST and LC data were downloaded from the MODIS website and elevation data were downloaded from the USGS website. The average increase in daytime LST per decade in Taiwan was 0.03 °C. The average accelerated increasing temperature was found 41.5% and those with accelerated decreasing trends accounted for 29% of the whole sub-regions. Daytime LST increase in the North at an elevation lower than 1,000 meters had a decreasing trend while the increasing trend was found at an elevation higher than 1,000 meters above sea level whereas daytime LST in the South at an elevation lower than 350 had a decreasing trend while the increasing trend was found at an elevation higher than 350 meters above sea level. Elevation and LC had significant affected the daytime LST increase with r square 18.9% for the North and 21.3% for the South of the country. The reasons for these differences need to be investigated in further studies.

Methods

The natural cubic spline method with eight knots assigned in this model, which were on the days 10, 40, 80, 130, 240, 290, 330 and 360 was used to model daytime LST annual seasonal patterns. The daytime LST was adjusted for seasonal patterns using least-squares regression in order to investigate the trends. Seasonally adjusted daytime LST were calculated by subtracting the original values with fitted values from the natural cubic spline and adding the mean values of each sub-region back to confirm that the average temperatures over the 20 years were not changed. The LST trends of all sub-regions were plotted on a Taiwan map in order to illustrate the different temperature trends for the whole country. All of the average increases of daytime LST from the 1,800 sub-regions were plotted against the accelerating increase in LST per decade. Linear regression was applied to predict the average increase of daytime LST based on elevation and LC. The coefficients from the model were converted to average daily increases of LST with 95% confidence intervals. Confidence interval graphs were created to illustrate the impact of elevation and LC on the increase in LST.

Results

Daytime LST seasonal adjusted and trends

Figure 1 Time series trends for corresponding seasonally-adjusted daytime LST in region 2 with 9 sub-regions

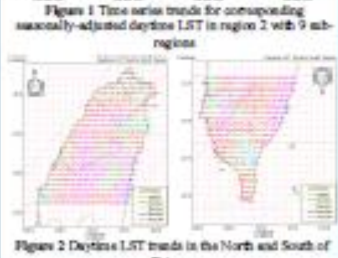

Figure 2 Daytime LST trends in the North and South of Taiwan

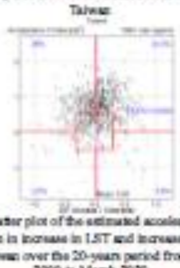

Fig. 3 Scatter plot of the estimated acceleration and deceleration in increase in LST and increase in daytime LST in Taiwan over the 20-years period from February 2000 to March 2020

Acknowledgement

We would like to thank the Royal Golden Jubilee Ph.D. program Scholarship under Thailand Science Research and Innovation (TSRI) and National Research Council of Thailand (NRCT) (Grant No. PHD/0205/2560). We acknowledge the Department of Research Methodology, Prince of Songkla University, Pattani campus, for providing facilities for this study. We are grateful to Professor Don McNeil for his immense guidance during the study.

Impact of elevation and LC on daytime LST increase

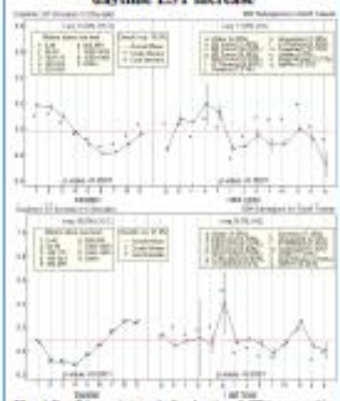

Fig. 4 Confidence intervals for daytime LST increased in all sub-regions in the North and South regions based on a linear regression model with elevation and LC as determinants

Discussion and Conclusion

The overall mean daytime LST increased by 0.03°C per decade. Moreover, our finding is inconsistent with the Council for Economic Planning and Development in Taiwan report (Council for Economic Planning and Development, 2012), which reported that Taiwan's temperature in the year 1980 to 2009 had increased by 0.29 °C per decade. In the North, daytime LST increase at an elevation less than 180 meters above sea level had significantly higher than the average while in the South, daytime LST increase at elevation greater than and equal to 1,000 meters had significantly higher than average. Daytime LST increase had shown an increasing trend in the past two decades. Daytime LST increase between the North and the South was influenced by elevation and LC differently. Other factors influencing the increase in LST apart from elevation and LC should be investigated in further studies in order to monitor anthropic climate change and to effectively control and manage land use and its effect on LST.

References

Council for Economic Planning and Development (2012). Adaptation Strategy to Climate Change in Taiwan. Taipei, 1st edition. ISBN: 978-986-03-3755-6

VITAE

Name Mr.Sahidan Abdulmana

Student ID 6020330010

Educational Attainment

Degree	Name of Institution	Year of Graduation
B.Sc. (Information Technology)	Yala Islamic University	2009
M.IT (Information Technology)	International Islamic University Malaysia	2012

Scholarship Awards during Enrolment

1. Royal Golden Jubilee (RGJ) Ph.D. program Scholarship under Thailand Science Research and Innovation (TSRI) and National Research Council of Thailand (NRCT) (Grant No. PHD/0205/2560).

Work – Position and Address

Lecturer

Department of Information Technology, Faculty of science and Technology, Fatoni University

List of Publication and Proceeding

Publications

Abdulmana, S., Lim, A., Wongsai, S. and Wongsai, N. 2021. Land surface temperature and vegetation cover changes and their relationships in Taiwan

from 2000 to 2020. Remote Sensing Applications: Society and Environment, 24, 100636.

Abdulmana, S., Lim, A. and Hama, I. 2021. Modeling vegetation index changes in Taiwan from 2000 to 2020. Malaysian Journal of Information and Communication Technology, *6*(2), 30-39.

Abdulmana, S. and Lim, A., Wongsai, N., Wongsai, S. 2021. Effect of land cover change and elevation on decadal trend of land surface temperature: a linear model with sum contrast analysis. Theoretical and Applied Climatology. (Under review)

Proceedings

Abdulmana, S. and Lim, A. 2019. Modeling for seasonal pattern and trend of land surface temperature in Taiwan. 62nd ISI World Statistics Congress 2019, Kuala Lumpur, Malaysia. August 18-23, 2019, 346-353.

Abdulmana, S. and Lim, A. 2021. Assessment of land surface temperature changes in Taiwan from 2000 to 2020. The 2021 National RGJ and RRI Conferences, Bangkok. June 14, 2021.

Abdulmana, S. and Lim, A. 2021. Impact of elevation and land cover on land surface temperature seasonal patterns and trends in Taiwan from 2000 -2020. Thailand Weather and Climate Symposium (TWCS-2021), Bangkok. December 16–17, 2021.